The Democratic People's Republic of Algeria

Ministry of Higher Education and Scientific Research

Thesis of End Studies

Presented at

Echahid Hamma Lakhdar University-El Oued

Faculty of Technology

Department of Electrical Engineering

In order to obtain a diploma with

ACADEMIC MASTER

Degree

In Telecommunications

Presented by

HATHROUBI Hadjer and MERAGHNI EL-Bachir

Theme

Design of ZBLAN photonic crystal fiber with nearly zero ultra-flattened chromatic dispersion

Defend at 26/05/2016. In front of the jury composed of:

Ms. BOUKAOUS Chahra	Associate professor	President
Mr. MEDJOURI Abdelkader	Associate professor	Rapporteur
Mr. HATTIRI Messaoud	Associate professor	Examiner

Academic Year 2015/2016

Appreciation

First of all, we start by addressing our most sincere thanks to our research promoter Mr. MEDJOURI Abdelkader, who has proposed this very interesting topic. This achievement could not be carried out in large part due to his kindness and cooperation. We are also grateful to him for his unfailing availability and dynamism during the entire duration of this thesis and to the scientific and pedagogical skills of it's frame without which this work would not have emerged.

Our thanks also go to our colleagues with whom we shared the section, finally many thanks to our parents and our families for their support.

Dedication

We dedicate this modest work:

To Our parents. May god give them good health and long life.

To our brothers and sisters,

For all family members and friends,

And to all those who contributed to the realization of this theses ,we say

thank you.

Abstract

The research work reported in this thesis deals with the analyzing and optimizing the linear and nonlinear properties of ZBLAN circular lattice photonic crystal fiber (CL-PCF), in the aim of their applications in optical telecommunications, also the different optical properties such as the confinement loss, the chromatic dispersion, the birefringence and the effective mode area are calculated and optimized by using the finite difference frequency domain method (FDFD). The simulations results shows that with optimizing their opto-geometrical parameters, the PCF can exhibit interesting properties that couldn't be achieved with conventional fibers. Considering the numerical modeling, by using the nonlinear Schrödinger equation (NLSE) to describe the pulses propagation within the PCF , we show the possibility of generating of supercontinuum by exploiting the nonlinear effects that occur during the propagation of ultra-short pulses (femtosecond) in the PCF.

Keywords

Photonic crystal fiber, ZBLAN, Finite difference method frequency domain, Nonlinear Schrödinger equation, supercontinuum generation.

Résumé

Le travail présenté dans ce mémoire concerne l'étude et l'optimisation des propriétés linéaires et non linaires des fibres optiques microstructurées (FOM) à base de ZBLAN trouée avec une configuration circulaire, en vue de leurs utilisations dans les systèmes de télécommunications optiques et les différentes propriétés des FOM telles que les pertes par confinement, la dispersion chromatique, la biréfringence et l'aire effective de mode sont analysées et optimisées en utilisant la méthode de différences finies dans le domaine fréquentiel FDFD. Les résultats de simulations montrent qu'avec une bonne optimisation de leurs paramètres opto-géométriques, les FOM peuvent présenter des propriétés de propagation singulières, inaccessibles aux fibres conventionnelles. La modélisation numérique, quant à elle, est basée sur la résolution de l'équation non linéaire de Schrödinger (NLSE), nous montrons la possibilité de générer des supercontinuums exploitant les effets non linéaires se manifestant dans les FOM lors de la propagation des impulsions ultra-courtes (femtoseconde).

Mots clés

Fibre optique microstructurées, ZBLAN, méthode de différences finies dans le domaine fréquentiel, Equation non linéaire de Schrödinger, génération du supercontinuum.

ملخص

هـذه المـذكرة تتنـاول دراسـة ونمذجـة الخصـائص الخطيـة و الغيـر خطيـة للأليـاف البصـرية ذات الكرسـتالات الضـوئية (PCF) بإسـتخدام زجـاج ZBLAN عوضـا عـن زجـاج السـيليس ، لهـدف تطبيقهـا فـي مجـال الإتصـالات البصـرية. وأيضـا دراسـة الخصـائص البصـرية المختلفـة مثـل ضـياع الطاقـة، والتشـتت اللـوني، والإنكسـار المزدوج و المسـاحة الفعليـة للـنمط التـي بـدورها تكـون محسـوبة و منمذجـة بإسـتخدام طريقـة الفـروق المحـدودة فـي المجـال الهرتـزي (التـرددي) FDFD. و أثبتـت نتـائج المحاكـاة أنـه مـع إختيار أمثـل لخصـائص الليـف البصـري ذات الطـابع الهندسـي، يمكـن لليـف البصـري أن يحمـل خصـائص مثيـرة للإهتمـام التـي لا يمكـن تحقيقهـا مـع الألياـف التقليديـة، بالإضـافة إلـى ذلـك إسـتخدمنا المعادلـة الغيـر الخطيـة لشـرودنغر (NLSE) لوصـف إنتشـار النبضـات داخـل الليـف البصـري مـن أجـل إنتـاج ضـوء واسـع الطيـف (supercontinuum) مـن خـلال إسـتغلال التـأثيرات الغيـر الخطيـة التـي تحـدث أثنـاء إنتشـار النبضـات القصـيرة جـدا (الفيمتـو ثانيـة) فـي الليـف البصري.

كلمات مفتاحية

ألياف البصرية ذات الكرستالات الضوئية , زجاج ZBLAN , طريقة الفروق المحدودة في المجال الهرتزي، المعادلة الغير الخطية لشرودنغر، إنتاج ضوء واسع الطيف.

List of contents

Chapter I: Introduction to photonic crystal fibers

Chapter II : Optical properties of photonic crystal fiber

Chapter III: Modeling results of ZBLAN PCF by the finite difference frequency domain method

List of figures

Chapter I

Chapter II

Chapter III

List of tables

Chapter I

Chapter II

Chapter III

Abbreviations and acronyms

AG	Air Guiding
BG	Band Gap
BPM	Beam Propagation Method
CLEO	Conference on Lasers and Electro Optics
CL-PCF	Circular Lattice Photonic Crystal Fiber
CW	Continuous Wave
DDF	Dispersion Decreasing Fiber
EMA	Effective Mode Area
ESM	Endlessly Single Mode
FD	Finite Difference
FDFD	The Finite Difference Frequency Domain
FDTD	The Finite Difference Time Domain
FEM	The Full Vector Finite Element method
FOM	Fibre Optique Microstructurée
FSM	Fundamental Space Cladding Mode
FTTH	Fiber To The Home
FWHM	Full Width At Half Maximum
GVD	Group Velocity Dispersion
HC	Hollow Core
HF	Holey Fibers
HIC	High Index Core
HNL	Highly Non Linear
HNQ	High Numerical Aperture
IG	Index Guiding
LBF	Localized Basis Functions
LMA	Large Mode Area
MI	Modulation Instability
MOF	Microstructured Optical Fiber
MPM	Multipole Method
MTIR	Modified Total Internal Reflection
OFC	Optical fiber Conference
PBG	Photonic Bandgap Guidance
PCF	Photonic Crystal Fibre

PWE	The Full Vector Plane Wave Expansion
QELS	Quantum Electronics and Laser Science Conference
SC	Supercontinuum Generation
SEM	Scanning Electron Microscope
SMF	Single Mode Fiber
TIR	Total Internal Reflection
UPML	Uniaxial Perfect Matching Layer
WDM	Wavelength Division Multiplexing

General Introduction

In telecommunications systems, the use of increasingly important optical fiber has enabled millions of users to access and transmit quantities of information simultaneously. To meet the growing demand of the quantity and flow of this information, the capacity of optical transmission systems can be read in two ways: either by increasing through by channel or by work simultaneous on multiple channels centered on different wavelengths (WDM). However, these two solutions are accompanied by a number of adverse effects. The first harmful phenomenon limiting the transmission rates is the chromatic dispersion reflects the fact that the group velocity in the guide is a function of wavelength.. The second source of degradation in telecommunications systems comes from nonlinear effects. These effects, which occur when the guided power densities are high, causing generation of frequencies causing cross-talk between channels. So we see that in order to increase transmission rates, it is necessary to design fibers whose propagation characteristics meet requirements becoming more stringent. The potential offered by the conventional fibers were widely exploited and their limitations were also well defined. It then proves necessary to pay attention to non-conventional optical fibers.

Since about ten years, the researches about a novels materials have open the possible to confine and to control the light in the cavities or wave guide through physics phenomenon as well known by photonic bandgap name , the discover of this effect give rise to members of applications and particularly of realization the component in optical fiber and more recently of realization novel generation of optical fiber .

In this context, photonic crystal fibers (PCF), consisting of an arrangement of air channels of micron parallel section to the direction of propagation in a pure silica matrix, are particularly attractive. Since their advent in the 1990s, PCF, aroused great interest, especially for their confinement capacity of light and the ability to tailor their design for provide dispersion at wavelength given. Indeed, adjusting the geometrical parameters of

PCF opened a vast field in the domain of engineering to optimize and to control the optical properties of the fiber.

The research reported in this thesis is analyzing the linear and nonlinear optical properties of ZBLAN CL-PCF for their uses in telecommunications systems. For this, we perform a series of numerical models, using the finite difference frequency domain method (FDFD) to optimize the various PCF properties, such as confinement losses, chromatic dispersion, birefringence and the effective area mode. In a second part, we study the spread ultra-short pulses (femtoseconds) in the PCF for the purpose of generating broad spectrum (supercontinuum).

The manuscript consists of three chapters:

In the 1st chapter we presented the structure of the PCF with its different opto geometrical parameter, then when mention the types of the fiber which can be classified by their guiding mechanism, the method of stack and draw that is used in fabrication process, in the end the different application of this fiber and the most important is supercontinuum generation which can be used in the domain of telecommunication as the wavelength-division multiplexed (WDM) systems.

In the 2nd chapter we presented the different characteristic, losses mechanism, chromatic dispersion, effective area and birefringence , in the end the different method than can be used in the modeling process , in our study we used The Finite Difference Frequency Domain method (FDFD) due to their general approach and describe arbitrary.

The 3th chapter, using the Lumerical and the FDFD method to optimize and analyze ZBLAN PCF large effective area in circular configuration. This chapter is also an opportunity to demonstrate the flexibility of the method of finite differences in optimization of both structures. For the circular configuration of PCF, offer a solution to reduce bending losses while keeping a sufficiently large effective area and reports the supercontinuum generation in PCF. In the first part, we describe the physical model with the different nonlinear effects contributing to its generation and the numerical model (Schrödinger Nonlinear equation "NLSE") used for simulation of the propagation of ultra-short pulses in optical fibers. In the second part, we present the results of numerical simulations on the supercontinuum generation in a PCF silica chromatic dispersion near zero and ultra-flat in PCF ZBLAN core suspended highly nonlinear and chromatic dispersion zero around the wavelength of 1.55 µm .

Chapter I

Introduction to photonic crystal fibers

I.1 Introduction

Until recently, an optical fiber was a solid thread surrounded by another material with a lower refractive index. Today, photonic crystal fibers (PCFs) are established as an alternative fiber technology. PCFs, which have been first demonstrated in 1995, are optical fibers with a periodic arrangement of low index material in a background with higher refractive index. The background material in PCFs is usually undoped silica and the low-index region is typically provided by air-holes running along their entire length.

In the first of this chapter, we will take a previous look of the PCF history then the structure and some of their geometrical parameters that's defined guiding mechanisms which given us the types of the photonic crystal fibers, After that we will mention the famous fabrication method of the photonic crystal fibers (Stack and Draw) .In the end we will take a look of its most used application.

I.2 Historic

Photonic crystals are today used as a general term describing periodic structures both in one, two, and three dimensions. While structures with a periodicity in one dimension (1D) have been known and exploited for decades, (e.g. finding use in high-reflection mirrors and fiber Bragg gratings), their two- and three-dimensional (2D and 3D) counterparts have only been explored since the publication of the original ideas of Yeh Yablonovitch and John in 1987.[1]

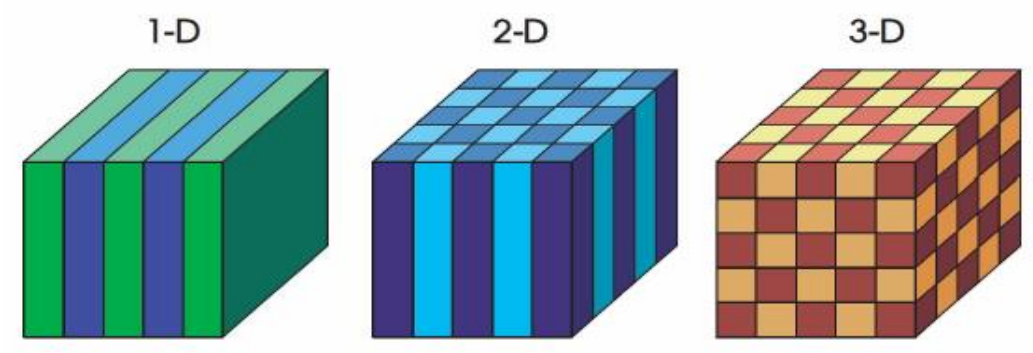

Fig I.1 : Examples for photonic crystals with 1, 2 and 3 dimensions. The different colors represent the materials with different index refractive.[2]

In 1991, Philip Russell, who was interested in Yablonovitch's research, got his big "crazy" idea for "something different," during CLEO/QELS conference. Russell's idea was that light could be trapped inside a fiber hollow core by creating a two-dimensional photonic crystal in the cladding, which is a periodic wavelength scale lattice of microscopic air holes in the glass. [3]

A photonic crystal fiber made of 2D photonic crystal with an air core was invented by P. Russell in 1992 and the first PCF was reported at the Optical Fiber Conference (OFC) in 1996 and is depicted in Fig.(I.2a) whereas the first hollow core PCF has been drawn in 1999 and can be found in Fig.(I.2b,c).[4]

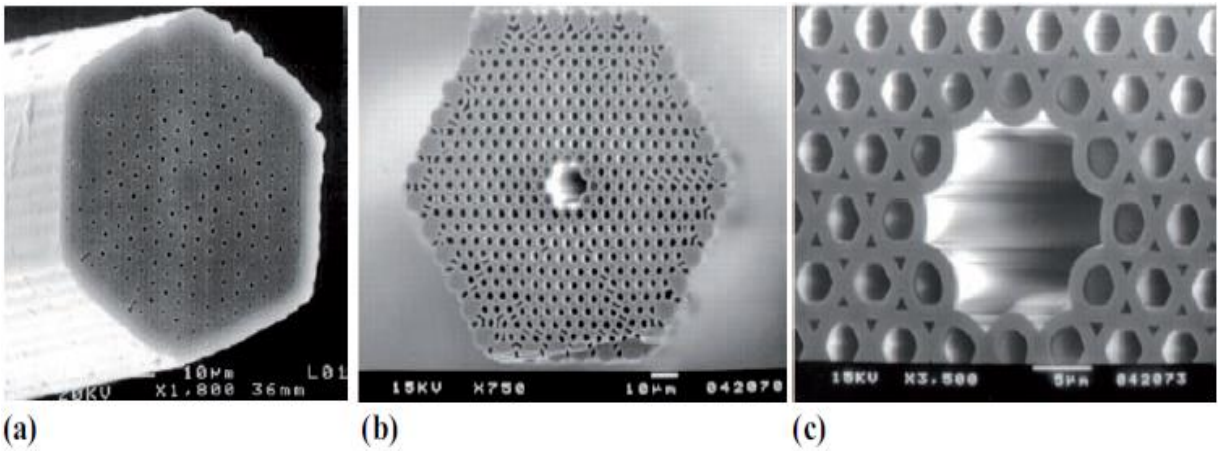

Fig I.2 :SEM image of the first solid core PCF , (b,c) SEM images of the first hollow core PCF.[4]

A short overview of PCF development is presented in the Table.

1978	Idea of the Bragg fiber
1992	Idea of the photonic crystal fiber with air core
1996	Fabrication of a single-mode fiber with photonic coating
1997	Endlessly single mode PCF
1999	PCF with photonic bandgap and air core
2000	Highly birefringent PCF
2000	Supercontinuum generation with PCF
2001	Fabrication of a Bragg fiber
2001	PCF laser with double cladding
2002	PCF with ultra-flattened dispersion
2003	Bragg fiber with silica and air core
2003	High puissance laser demonstration use the PCF
2004	Supercontinuum generation in the PCF with two zeros dispersion
2006	High pression reactor realization basis of PCF
2007	Chalcogenures PCF demonstration for non-linear Applications
2008	Supercontinuum generation in PCF with full water core

Tab I.1: Overview of photonic crystal fibers development. [5, 6]

I.3 Structure of the photonic crystal fiber (PCF)

Photonic crystal fibers (PCFs) are fibers with an internal periodic structure made of capillaries, filled with air, laid to form a hexagonal (circular, triangular...) lattice. Light can propagate along the fiber in defects of its crystal structure. A defect is realized by removing one or more central capillaries.

PCFs are principally defined by three key parameters as shown in Fig. I.3 the center to center separation of the cladding inclusions (either air holes or doped glasses) the pitch Λ, the diameter of the cladding inclusions d, and the core diameter d_c defined as the shortest distance across the core between the closest spaced cladding inclusions.[5,7]

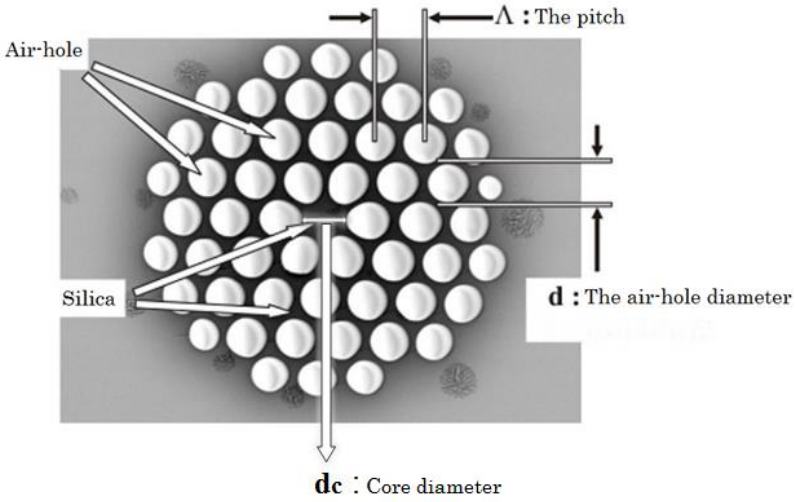

Fig I.3 : Cross-section of a PCF with hexagonal structure.[8]

I.4 Guiding mechanisms

In order to form a guided mode in an optical fiber, it is necessary to introduce light into the core with a value of β, which is the component of the propagation constant along the fiber axis, which cannot propagate in the cladding. The highest β value that can exist in an infinite homogeneous medium with refractive index n is $\beta = nk_0$,being k_0 the free space propagation constant. All the smaller values of β are allowed. A two-dimensional photonic crystal, like any other material, is characterized by a maximum value of β which can propagate. At a particular wavelength, this corresponds to the fundamental mode of an infinite slab of the material, and this β value defines the effective refractive index of the material. [3]

I.4.1 Modified total internal reflection guidance (MTIR)

It is possible to use a two-dimensional photonic crystal as a fiber cladding, by choosing a core material with a higher refractive index than the cladding refractive index. These fibers, also known as index guiding PCFs, guide light through a form of total internal reflection (TIR), called modified TIR. However, they have many different properties with respect to conventional optical fibers. [3]

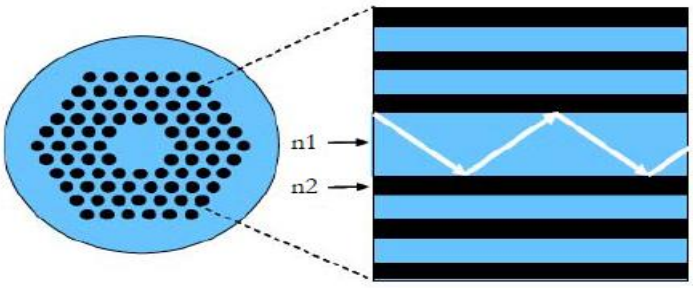

Fig I.4 : Guiding with MTIR, n_1=1.45(silica) and n_2=1(air) (blue=silica, black=air) .[6]

Index guiding fibers are characterized by an average refractive index of the core region higher than that of the cladding. By far the most common type of PCF is the large mode area or LMA fiber the cross section and mode of which is shown in Fig.5 (a) and (b).

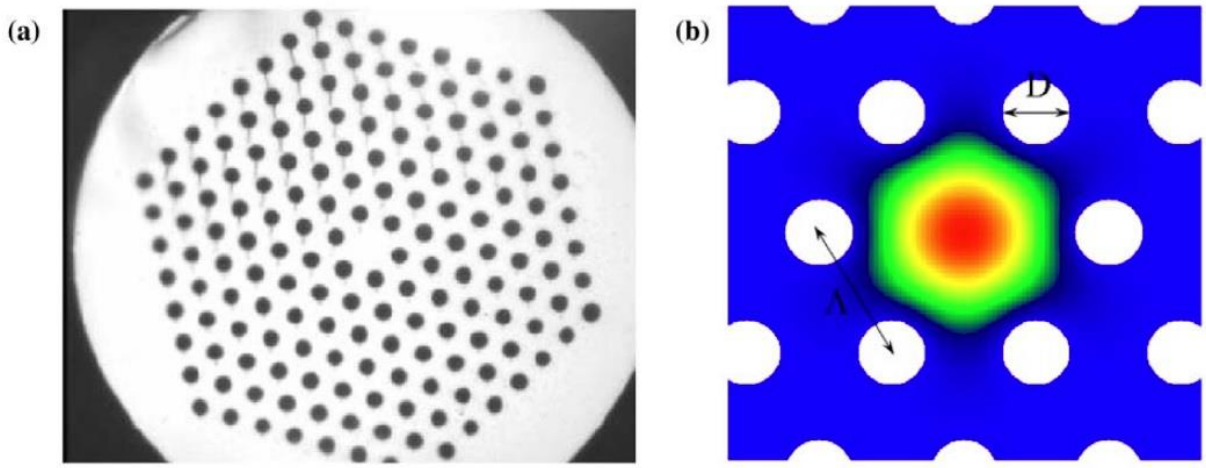

Fig I.5 : ***(a)*** *Cross section of an LMA fiber (Crystal Fiber A/S).* ***(b)*** *The geometric layout and mode field distribution.*[9]

All guided modes in a traditional step index fiber must satisfy the relationship:

$$n_{co} > \frac{k_z}{k} > n_{cl} \tag{I.1}$$

This inequality is derived from the fact that each mode travels along the fiber with a phase velocity defined by $\frac{kz}{k} = \frac{c}{v}$.It is unphysical that the phase velocity of the mode is less than the local speed of light in the core and whilst v_{mode} can exceed v_{cl} ,this physically means that energy within the cladding is being lost from the mode by radiation and hence the mode is no longer strictly bound and so any fully bound mode must satisfy the relationship $v_{cl} > v_{mode} > v_{co}$ from which (I.1) is derived. The higher core refractive index forces at least one index guided mode to appear between the core and cladding refractive indices. The cladding is seen to behave as a region of homogeneous material with lower refractive index than the core .Thus index guiding fibers are thus characterized by a core refractive index higher than that of the cladding. The V value may be defined for an LMA fiber in much the same manner as a step index fiber with:

$$V_{step} = ka\sqrt{n_{co}^2 - n_{cl}^2} \tag{I.2}$$

$$V_{LMA} = k\Lambda\sqrt{n_{co}^2(\lambda) - n_{cl}^2(\lambda)} \tag{I.3}$$

In the step index case for a given core radius, a and numerical aperture

$$NA = \sqrt{n_{co}^2 - n_{cl}^2} \tag{I.4}$$

$V_{step} \propto \lambda^{-1}$ any increase in a for the same k will increase the number of mode that can, in some sense, fit within a and so as the value of V increases so the number of modes supported increases. In the lower limit, a single-mode cutoff at $V_{step} = 2.405$ exists below which only the fiber fundamental mode can propagate. [9]

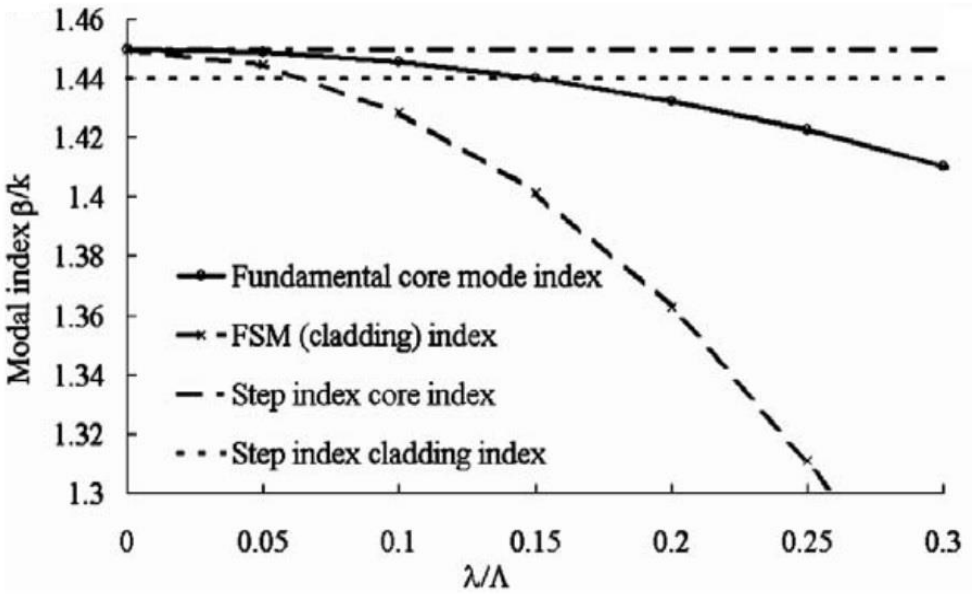

Fig I.6 : Modal indices of the LMA fundamental core mode and fundamental space filling (cladding) mode as function of k for a fiber of $d/K = 0.40$. The core and cladding refractive indices of a step-index fiber are shown (without material dispersion) for comparison. [9]

I.4.2 Photonic bandgap guidance (PBG)

Optical fiber designs completely different form the traditional ones result from the fact that the photonic crystal cladding have gaps in the ranges of the supported modal index $\frac{\beta}{k_0}$ where there are no propagating modes. These are the PBGs of the crystal, which are similar to the two-dimensional band gaps which characterize planar light wave circuits, but in this case they have propagation with a non-zero value of β. It is important to underline that gaps can appear for values of modal index both greater and smaller than unity, enabling the formation of hollow core fibers with bandgap material as a cladding, These fibers, which cannot be made using conventional optics, are related to Bragg fibers, since they do not rely on TIR to guide light. In fact, in order to guide light by TIR, it is necessary a lower-index cladding material surrounding the core, but there are no suitable low loss materials with a refractive index lower than air at optical frequencies. The first PCF which exploited the PBG effect to guide light was reported in 1998; Notice that its core is formed by an additional air hole in a honeycomb lattice. This PCF could only guide light in silica, which is in the higher-index material.

Hollow core guidance had to wait until 1999, when the PCF fabrication technology had advanced to the point where larger air filling fractions, required to achieve a PBG for air-guiding, became possible. Notice that an air guided mode must have $\frac{\beta}{k_0} < 1$, since this condition guarantees that light is free to propagate and form a mode within the hollow core, while being unable to escape into the cladding.

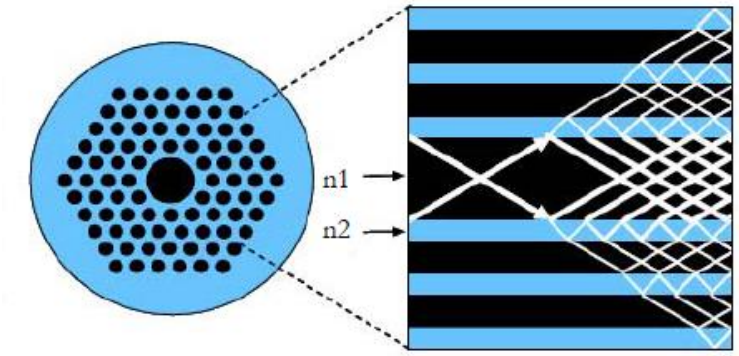

Fig I.7 : Guiding with PBG, n_1=1(air) and n_2=1.45 (silica) (blue=silica, black=air). [6]

The first hollow core PCF had a simple triangular lattice of air holes, and the core was formed by removing seven capillaries in the center of the fiber cross section. By producing a relatively large core, the chances of finding a guided mode were improved. When white light is launched into the fiber core, colored modes are transmitted, thus indicating that light guiding exists only in restricted wavelength ranges, which coincide with the photonic bandgap. [3]

Any PCF or microstructured fiber may be placed in one of two main classes, namely either fibers operating by a principle comparable to that of standard optical fibers with a total internal reflection (TIR), or those guiding light by the photonic bandgap (PBG) effect. The fibers belonging to the first main class may often be referred to as High-Index Core (HIC) fibers, Index-Guiding (IG) fibers, or Holey Fibers (HF). In the second main class, the fibers are generally referred to as PBG fibers or Bandgap-Guiding (BG) fibers.

We may now divide each of the two main classes into a number of subclasses, which primarily are determined by the dimensions of the fiber structures, and their specific properties. For the index-guiding fibers, three subclasses have today immerged, and they are as follows:

- Large-Mode-Area (LMA) fibers using relatively large dimensions and small effective refractive index contrasts to spread out the transverse optical field. Fig 1.8 (a)

- Highly-Non-Linear (HNL) fibers that applies very small core dimensions to provide tight mode confinement. Fig 1.8 (b).
- High Numerical Aperture (HNA) fibers having a central part surrounded by a ring of relatively large air-holes. Fig 1.8 (c).

The photonic bandgap fibers may be separated into the sub-classes of :

- Air-Guiding (AG) or Hollow-Core (HC) fibers. Fig 1.8 (d).
- The rotation symmetrical Bragg fibers .Fig 1.8 (e).

Although the latter with its ring structure is somewhat different from the rest of the fibers having individual holes/voids distributed in the cladding. Although the effective refractive index of the core region is lower than that of the cladding region, the major part of the optical power is propagating in the high index material (most commonly the silica).

In contrast to this, the air-guiding fibers provide a bandgap, which allow the majority of the optical power to propagate in the central hole of the fiber structure and hereby the name air guiding naturally appears. [1]

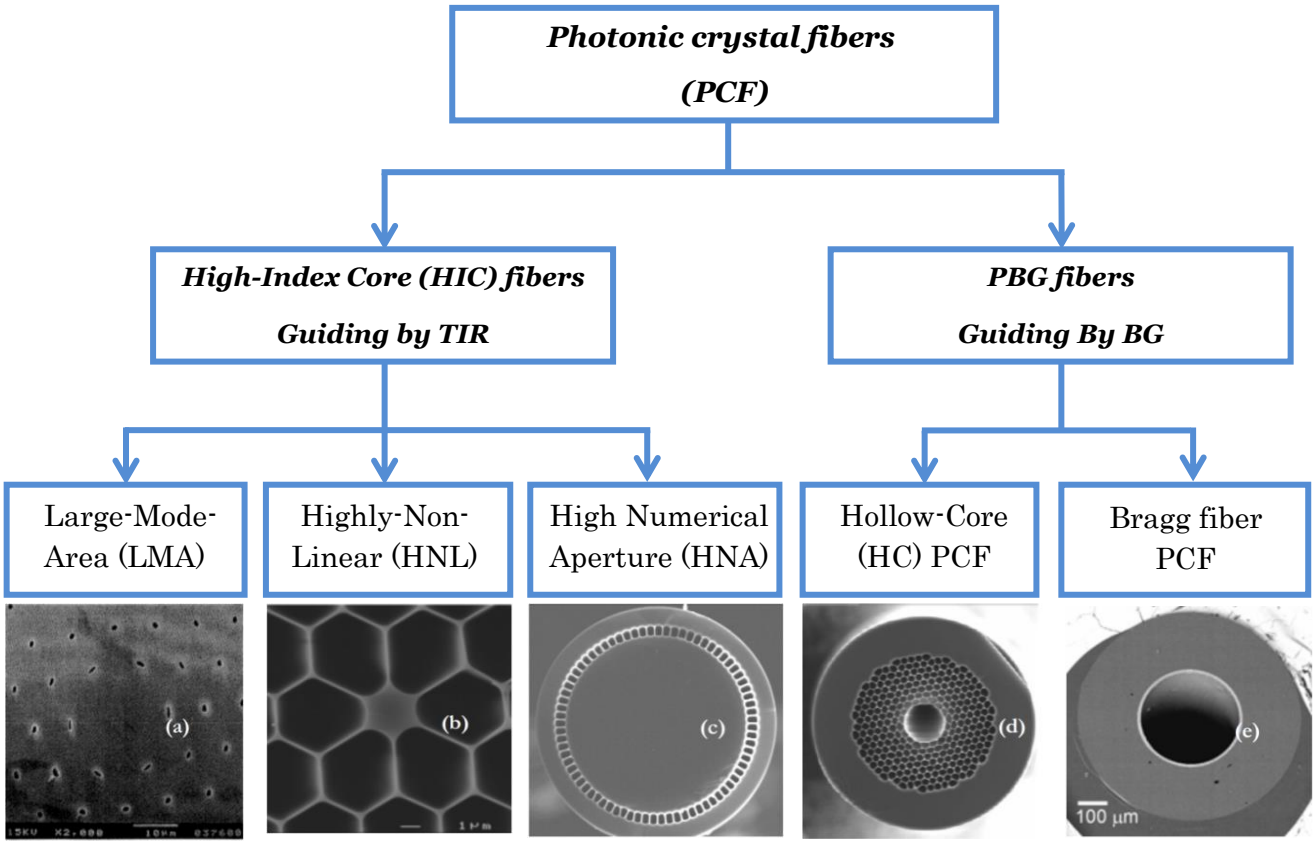

Fig I.8 : Classification of PCF according to their guiding mechanisms.[6]

I.5 Fabrication of PCF's

Fabrication of both PCF and conventional optical fiber requires first the creation of a macroscopic preform of the desired microscopic fiber structure. These preforms are then drawn to fiber on a fiber drawing tower in a similar manner to the fabrication of seaside rock. There are a number of ways of fabricating PCF preforms, with the most common being the stack and draw method (Fig I.9).

First, capillaries are drawn from glass tubes and then stacked in a close packed array with any solid defects (such as the core) created by the replacement of a capillary with a solid rod. This "stack" is then inserted into a tube (typically 20-25mm in diameter), and put on a fiber drawing tower, and drawn down to the preforms (typically 1-4 mm in diameter). These preforms provide a useful intermediate stage before drawing to fiber. The holes in the preforms are generally pressurized as they are drawn to fiber.

This can maintain the structure, or allow the holes to collapse or to be inated. It is even possible to apply different pressures to different holes by inserting capillaries into them and pressurizing the capillaries; this technique has been used to make polarization-maintaining PCFs. [7]

PCF preforms can also be created by drilling the desired structure into a solid rod. This technique not only limits the length of the preforms by the length of the drill bit, but also requires the silica cladding web to be thick walled in order to prevent the walls from breaking.

PCFs fabricated from soft glasses such as tellurite have also been reported. Here, the lower melting point of the glass allows preforms to be fabricated by extruding pellets of the glass through a metal die. [7]

A very important issue is the comparison of the PCF stack and draw procedure with the vapor deposition methods usually employed for standard optical fibers.

Obviously, it is more difficult that the preforms for conventional optical fibers become contaminated, since their surface area is smaller. Moreover, that temperature around 2100^{o} C, a lower temperature level, that is 1900^{o} C,

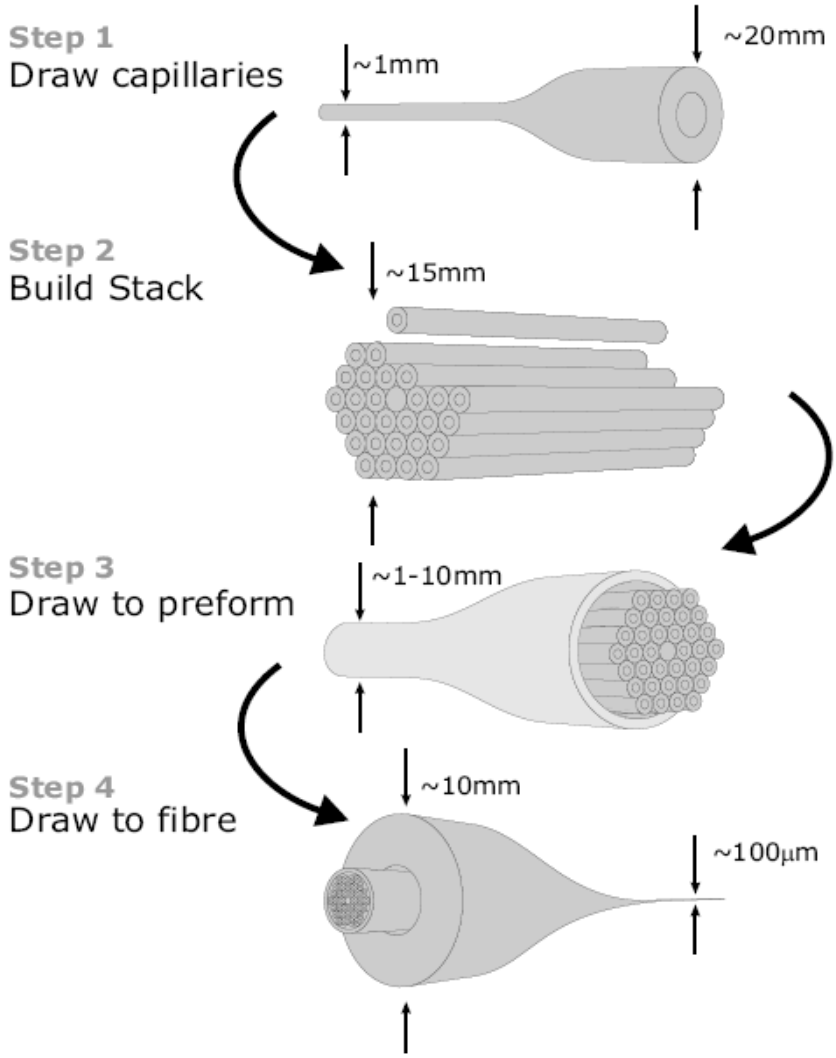

Fig I.9 ***:*** *A schematic representation of the stack and draw method of PCF fabrication. First, capillaries are drawn from pure silica tubes* ***(1)*** *and are then stacked in a close packed array with the introduction of a defect region to form the core* ***(2)****. These are drawn down to preforms* ***(3)*** *which are then jacketed in a silica tube and drawn to fiber****(4)****.*[7]

I.6 Applications

The diversity of new or improved features beyond conventional fibers means that PCFs are finding an increasing number of applications in ever-widening areas of science and technology.

I.6.1 High power and energy transmission

ESM-PCF's ability to remain single mode at all wavelengths where it guides, and for all scales of structure, suggests that it should have superior power — handling properties — the core area can be increased without the penalty of introducing higher order guided modes . The ability to transmit much higher power in a single mode has a major impact in the field of laser machining and high-power fiber lasers and amplifiers.

The key issue is bend loss, it turns out that PCF offers a wider bandwidth of useful single-mode guidance than high Δ-SMF, because it can operate in the multimode regime of SMF while remaining single mode. This also allows the long-wavelength bend edge to be moved to longer wavelengths.

Hollow core PCF is also an excellent candidate for transmitting high continuous wave power as well as ultra-short pulses with very high peak powers. Solitons have been reported at 1550 nm with durations of 100 fs and peak powers of 2 MW and at 800 nm using a Ti:sapphire laser. The soliton energy is, of course, determined by the effective value of γ and the magnitude of the anomalous GVD. [10]

I.6.2 Fiber lasers and amplifiers

PCF lasers can be straight forwardly produced by incorporating a rare earth doped cane in the preform stack. Many different designs can be realized such as cores with ultra large mode areas for high power and structures with multiple lasing cores.

Cladding pumping geometries for ultrahigh power can be fashioned by incorporating a second core (much larger and multimode) around a large off center ESM lasing core. Using microstructuring techniques, this "inner cladding waveguide" can be suspended by connecting it to an outer glass tube with very thin webs of glass. This results in a very large effective index step and, thus, a high numerical aperture (> 0.9), making it easy to launch and guide light from high power diode-bar pump lasers, which typically have poor beam quality. The multimode pump light is efficiently absorbed by the lasing core, and high power single mode operation can be achieved.

Hollow core PCF, with its superior power handling and designable GVD, is ideal as the last compression stage in chirped pulse amplification schemes. This permits operation at power densities that would destroy conventional glass core fibers. [10]

I.6.3 Intra-fiber devices cutting and joining

As PCF becomes more widely used, there is an increasing need for effective cleaves low loss splices, multiport couplers, intra-fiber devices, and mode area transformers. The air holes provide an opportunity not available in standard fibers: the creation of dramatic morphological changes by altering the hole size by collapse (under surface tension) or inflation (under internal overpressure) when heating to the softening temperature of the glass. Thus, not only can the fiber be stretched locally to reduce its cross sectional area, but also, the microstructure can itself be radically altered.

1. ***Cleaving and splicing:*** PCFs cleave cleanly using standard tools, showing slight end face distortion only when the core crystal is extremely small (inter hole spacing ~1 μm) and the air filling fraction is very high (> 50%). Solid glass end caps can be formed by collapsing the holes (or filling them with sol–gel glass) at the fiber end to form a coreless structure through which light can be launched into the fiber. A solid core PCF can be fusion spliced successfully both to it and to step index fiber using resistive heating elements (electric arcs do not allow sufficient control).

2. ***Mode transformers:*** In many applications, it is important to be able to change the mode area without losing light. This is done traditionally using miniature bulk optics tiny lenses precisely designed to match to a desired numerical aperture and spot size. In PCFs, an equivalent effect can be obtained by scanning a heat source (flame or carbon dioxide laser) along the fiber.

3. ***In-Fiber devices:*** Precise use of heat and pressure induces large changes in the optical characteristics of PCFs, giving rise to a whole family of new intra-fiber components. Micro couplers can be made in a PCF with two optically isolated cores by collapsing the holes to allow the mode fields to expand and interact with each other, creating local coupling .[10]

I.6.4 Kerr-related nonlinear effects

1. ***Parametric amplifiers and oscillators:*** In step index fibers, the performance of optical parametric oscillators and amplifiers is severely constrained owing to the limited scope for GVD engineering. In PCFs, these constraints are lifted, permitting flattening of the dispersion profile and control of higher order dispersion terms.

2. ***Supercontinuum generation:*** One of the most successful applications of nonlinear PCF is to SC generation from picosecond and femtosecond laser pulses. When high power pulses travel through a material, their frequency spectrum can be broadened by a range of interconnected nonlinear effects. In bulk materials, the preferred pump laser is a regeneratively amplified Ti:sapphire system producing high energy (in milli joules) femto second pulses at 800 nm wavelength and kilohertz repetition rate.

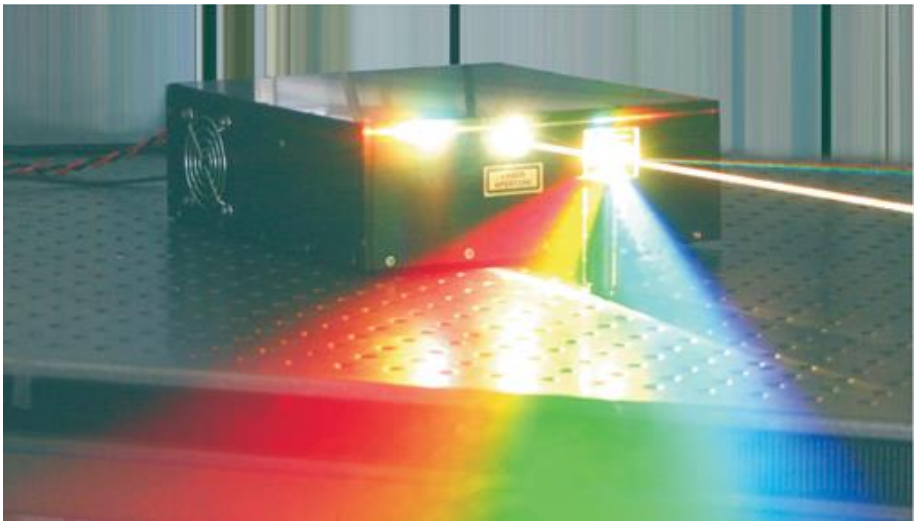

Fig I.10 : SC light generated in ESM-PCF from picosecond fiber laser. Total SC power is 6.5 W for a 10-W pump power (5-ps pulses). Repetition rate is 50 MHz, and the average spectral power density in the range 450–800 nm is a remarkable 4.5 mW/nm .[10]

3. ***Correlated photon pairs:*** The use of self-phase modulation to generate bright sources of correlated photon pairs is unsuccessful in step index fibers due to high Raman-related noise. This is because for $\beta_2 < 0$ and $\beta_n = 0, n > 2$, the modulational instability sidebands are situated very close to the pump frequency within the Raman gain band of the glass.

4. ***Soliton self-frequency shift cancellation:*** The ability to create PCFs with negative dispersion slope at the zero dispersion wavelength (in SMFs, the slope is positive, the dispersion becomes more anomalous as the wavelength increases) has made it possible to observe Čerenkov like effects in which solitons (which form on the anomalous side of the dispersion zero) shed power into dispersive radiation at longer wavelengths on the normal side of the dispersion zero.

This occurs because higher order dispersion causes the edges of the soliton spectrum to phase match to linear waves. The result is the stabilization of the soliton self-frequency shift at the cost of gradual loss of soliton energy. The behavior of solitons in the presence of wavelength-dependent dispersion is the subject of many recent studies. [10]

I.6.5 Brillouin scattering

The periodic micro/nano structuring in ultra-small core glass air PCFs strongly alters the acoustic properties compared to conventional SMFs. Sound can be guided in the core both as leaky and as tightly confined acoustic modes.

In addition, the complex geometry and "hard" boundaries cause coupling between all three displacement components (radial, azimuthal, and axial), with the result that each acoustic mode has elements of both shear or longitudinal strain. This complex acoustic behavior strongly alters the characteristics of forward and backward Brillouin scattering. [10]

I.6.6 Gas-based nonlinear optics

The diffraction of light beams in free space presents an apparently insuperable barrier to achieving efficient nonlinear interactions between laser light and low density media such as gases. The requirements of high intensity, long interaction length, and good quality (preferably single mode) transverse beam profiles simply cannot be met. A structure conceptually capable of delivering all these requirements simultaneously would be a perfectly guiding hollow-core waveguide supporting a single transverse mode with low attenuation losses. [10]

1. ***Stimulated raman scattering:*** In 2002, stimulated Raman scattering was reported in a hydrogen filled hollow core PCF at threshold pulse energies ~100× lower than previously possible. More recently, the threshold power for rotational Raman scattering in hydrogen was reduced by more than a million times in single-pass geometry, and near perfect quantum efficiency was achieved .Such gas cells have been hermetically spliced to standard all solid glass SMFs.

The limited wavelength ranges of guidance in hollow core are used to advantage here, making it possible to suppress the normally dominant vibrational Raman signal from hydrogen, and enhance the rotational Raman signal. [10]

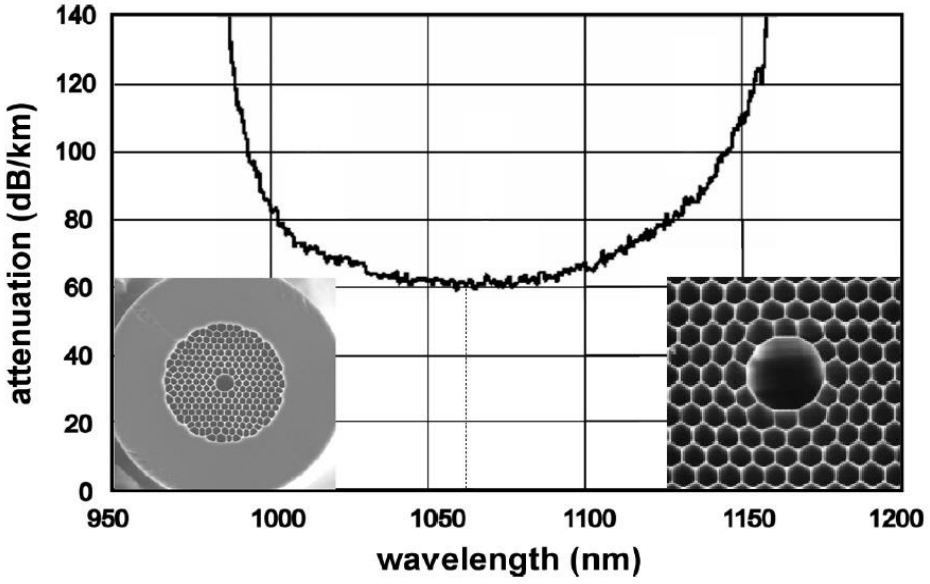

Fig I.11 : Attenuation spectrum of a hollow-core PCF designed for low-loss transmission of 1064 nm light. [10]

2. ***High harmonic generation:*** Hollow core PCF is likely to have a major impact in other areas of nonlinear optics, such as x-ray generation in noble gases pumped by fs Ti:sapphire laser pulses. The conversion efficiency of this process could be further enhanced by modulating the bore diameter of the core so as to phase match the light and the x-rays (this was recently demonstrated in simple glass capillaries). In a hollow core PCF this could be implemented for example by heat treatment with carbon dioxide laser light. [10]

I.6.7 Telecommunications

There are many potential applications of PCFs or PCF based devices in telecommunications, although whether these will be adopted remains an open question. One application that seems quite close to being implemented is the use of solid-core PCF or "hole-assisted" SMF for Fiber To The Home (FTTH), where the lower bend loss is the attractive additional advantage offered by the holey structure.

Other possibilities include dispersion-compensating fiber and hollow core PCF for long haul transmission. Additional opportunities exist in producing bright sources of correlated photon pairs for quantum cryptography, parametric amplifiers with improved characteristics, highly nonlinear fiber for all optical switching and amplification, acetylene filled hollow core PCF for frequency stabilization at 1550 nm, and the use of sliced SC spectra as WDM channels. There are also many possibilities for ultra-stable in line devices based on permanent morphological changes in the local holey structure induced by heating, collapse, stretching, or inflation. [10]

1. ***New telecommunications window:*** Hollow core PCF is radically different from solid core SMF in many ways. This makes it difficult to predict whether it could be successfully used in long haul telecommunications as a realistic competitor for SMF-28. The much lower Kerr nonlinearities mean that WDM channels can be much more tightly packed without nonlinear crosstalk, and the higher power handling characteristics mean that more overall power can be transmitted. The effective absence of bend losses is also a significant advantage, particularly for short-haul applications. [10]

2. ***Dispersion compensation:*** The large glass air refractive index difference makes it possible to design and fabricate PCFs with high levels of GVD. A PCF version of the classical W-profile dispersion compensating fiber was recently reported, offering slope matched dispersion compensation for SMF-28 fiber at least over the entire C-band (Fig. I.12).

Dispersion values of −1200 ps/nm.km imply that only 1 km of fiber is needed to compensate for 80 km of SMF-28. The fiber was made deliberately birefringent to allow control of polarization mode dispersion.

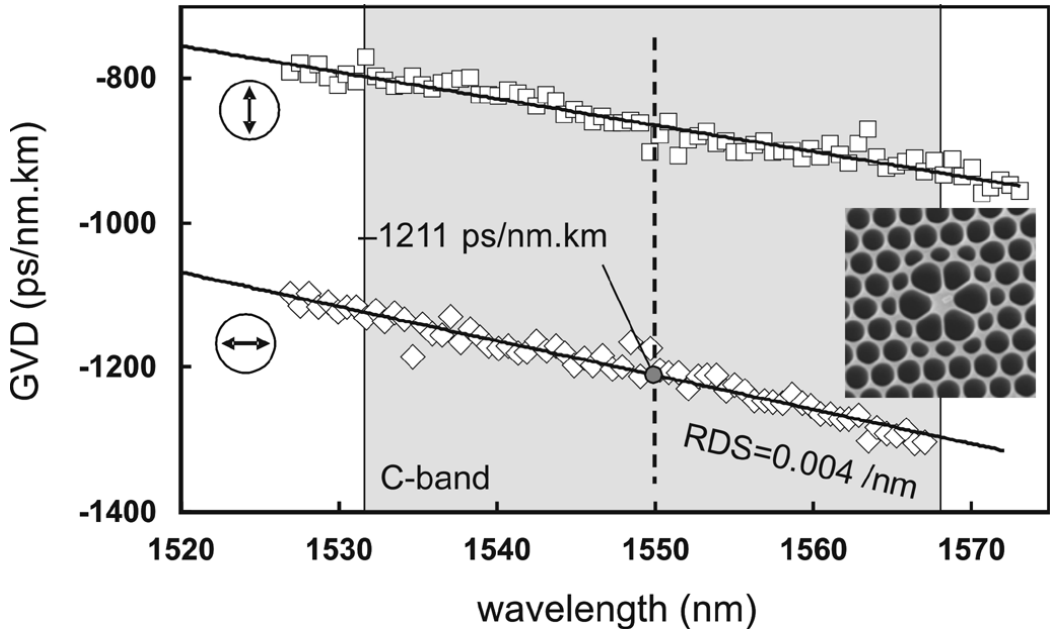

Fig I.12 : Performance of a PCF designed to provide slope-matched dispersion compensation for Corning SMF-28 over the C-band.[10]

I.6.8 laser tweezers in hollow core PCF

A focused light beam produces both a longitudinal (accelerating) and a transverse (trapping) force on dielectric micro particles. For maximum trapping force, the intensity gradient of the light must be as high as possible. This can be achieved by focusing a high power laser beam with a high numerical aperture lens. The Rayleigh length for such a tightly focused beam is rather short; furthermore, the high intensity will quickly accelerate the particle out of the trapping zone. Stable trapping of a particle in free space requires the longitudinal force to be balanced either by gravity or by a second (or reflected) beam. [10]

I.6.9 Optical sensors

Sensing is thus far a relatively unexplored area for PCFs, although the opportunities are myriad, spanning many fields including environmental monitoring, biomedical sensing, and structural monitoring .Multicore PCF has been used in bend and shape sensing and Doppler difference velocimetry , double clad PCF in multi photon fluorescence measurements in medicine , and solid core PCF for hydrostatic pressure sensing .[10]

I.7 Conclusion

At the moment, it can be expected that PCFs for higher power next generation fiber lasers and amplifiers and for supercontinuum generation will be the first products to reach the "real" market that is to gain commercial opportunities also outside the academic world. In fact, even if PCFs were originally envisioned as a solution for higher data rates in telecommunications, conventional optical fibers currently in use are so good that PCFs do not offer an obvious advantage right now.

References

[1] Anders Bjarklev, JesBroeng, Araceli Sanchez Bjarklev (auth*.), "Photonic Crystal Fibers, Springer" US (2003).*

[2] Aurélie Bétourné, ''*Conception et Caractérisation de Nouvelles Fibres Optiques à Cristal Photonique dites Hybrides et Applications à l'Optique Non Linéaire '',* PhD thesis, university Lille 1.

[3] Federica Poli, Annamaria Cucinotta, and Stefano Selleri", *Photonic crystal fibers: properties and applications, Springer (2007)".*

[4] Birgit Stiller,"Brillouin *scattering in photonic crystal fiber:from fundamentals to fiber optic sensors*, "PhD thesis, Université de Franche-Comté ,2011.

[5] R. Buczynski,"*Photonic Crystal Fibers* ", Proceedings of the XXXIII International School of Semiconducting Compounds, Jaszowiec 2004.

[6] Rim CHERIF, ''*Étude des Effets Non-Linéaires dans les Fibres à Cristaux Photoniques*, PhD thesis, university of 7 Novembre à Carthage, 2009 ''.

[7] James Morgan Stone, "*PHOTONIC CRYSTAL FIBRES AND THEIR APPLICATIONS IN THE NONLINEAR REGIME*», PhD thesis, University of Bath, April 2009.

[8] Melle Benaissa Fatima, ''*Etude et Simulation des Ondes Electromagnétiques dans les guides d'Ondes à Cristaux Photoniques-Application aux Fibres Optiques '',* Magister thesis university of ABOU-BAKR BELKAÏD – TLEMCEN, 2013.

[9] Jason C.W. Corbett, "*A brief introduction to photonic crystal fibers for astronomical instrumentalists",* Elsevier B.V.2006.

[10] Philip St .J. Russell, *"Photonic-Crystal Fibers*, JOURNAL OF LIGHTWAVE TECHNOLOGY, VOL. 24, NO. 12, DECEMBER 2006 ".

Chapter II

Optical properties of photonic crystal fiber

II.1 Introduction

Photonic crystal fiber is a new different type of optical fiber , so they can be defined by a different characterization, in this chapter we will take a general look about his optical proprieties such as the endlessly single mode, effective area, birefringence, chromatic dispersion, and loss mechanisms witch contents intrinsic loss (absorption, scattering), confinement loss and bending loss. In the end, we will mention the different modeling methods for PCF and we interested about finite difference frequency domain (FDFD) method.

II.2 PCF optical properties

II.2.1 Endlessly single mode property

The first solid core PCF (Fig I.2), which consisted of a triangular lattice of air holes with a diameter d of about 300 nm and a hole to hole spacing Λ of 2.3 µm, did not ever seem to become multi-mode in the experiments, even for short wavelengths. In fact, the guided mode always had a single strong central lobe filling the core.

Russell has explained that this particular endlessly single mode behavior can be understood by viewing the air hole lattice as a modal filter or "sieve" .Since light is evanescent in air, the air-holes act like strong barriers, so they are the "wire mesh" of the sieve. The field of the fundamental mode, which fits into the silica core with a single lobe of diameter between zeros slightly equal to 2Λ, is the "grain of rice" which cannot escape through the wire mesh, being the silica gaps between the air holes belonging to the first ring around the core too narrow. On the contrary, the lobe dimensions for the higher-order modes are smaller, so they can slip between the gaps. When the ratio d/Λ, that is the air filling fraction of the photonic crystal cladding, increases, successive higher order modes become trapped. A proper geometry design of the fiber cross section thus guarantees that only the fundamental mode is guided. More detailed studies of the properties of triangular PCFs have shown that this occurs for $d/\Lambda < 0.4$.

By exploiting this property, it is possible to design very large mode area fibers, which can be successfully employed for high power delivery, amplifiers, and lasers. Moreover, by doping the core in order to slightly reduce its refractive index, light guiding can be turned off completely at wavelengths shorter than a certain threshold value. [1]

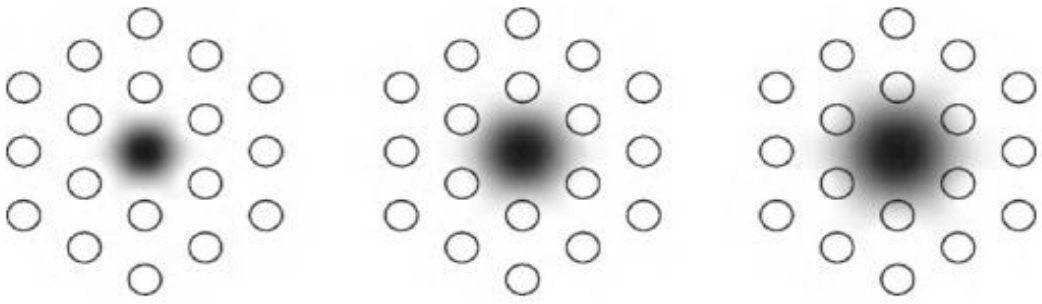

Fig II.1: The above schematics show how light penetrates into the cladding air holes for different wavelengths. The wavelength of light increases from left to right. The effective or average index of the cladding is reduced at longer wavelengths due to the field increasingly occupying the air regions. [2]

II.2.2 Chromatic dispersion

The effective refractive index of a confined mode in a fiber varies as a function of frequency w . The individual speeds experienced by different frequencies are different given by $\frac{c}{n(w)}$. Consider an optical pulse envelope propagating with several frequencies travelling at different speeds. The pulse envelope will spread out as it propagates, as the slower frequencies lag behind the faster ones; this process is known as chromatic dispersion. [3]

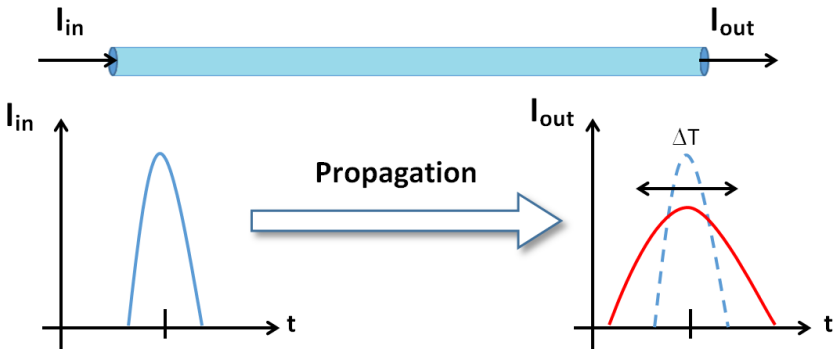

Fig II.2: Chromatic dispersion in the optical fiber. [4]

To describe chromatic dispersion of a pulse propagating in an optical fiber, a Taylor expansion of is taken around the central frequency of the pulse, w_0, to give

$$\beta(w) = n(w)\frac{w}{c} = \beta_0 + \beta_1(w - w_0) + \frac{1}{2}\beta_2(w - w_0)^2 + \frac{1}{6}\beta_3(w - w_0)^3 + \cdots \qquad \text{(II.1)}$$

Where

$$\beta_m = \left(\frac{d^m\beta}{dw^m}\right)_{w=w_0} \qquad m = 0, 1, 2, 3 \ldots\ldots \qquad \text{(II.2)}$$

The coefficients β_1 and β_2 are related to the refractive index and its derivatives through the relations:

$$\beta_1 = \frac{1}{v_g} = \frac{n_g}{c} = \frac{1}{c}\left(n + w\frac{dn}{dw}\right) \qquad \text{(II.3)}$$

$$\beta_2 = \frac{1}{c}\left(2\frac{dn}{dw} + w\frac{d^2n}{dw^2}\right) \qquad \text{(II.4)}$$

Where v_g is the group velocity and n_g is the group index. It can easily be seen from II.3 that the group index can be readily obtained from the second term of II.1.

Throughout this thesis we will refer to n_g and n as functions of wavelength. The parameter n_g varies as a function of n through the relation

$$n_g(\lambda) = n(\lambda) - \lambda \frac{dn(\lambda)}{d\lambda} \tag{II.5}$$

The coefficient β_2 determines how the individual frequencies in a pulse envelope disperse as it propagates. This is known as group velocity dispersion (GVD) and it is quantified by β_2, which is generally given in units of ps^2km^{-1}.

Dispersion is also quantified by the dispersion parameter, D, which has arisen for practical engineering use and has units of picoseconds of spreading per nanometre of bandwidth per kilometer travelled, ps $nm^{-1}km^{-1}$. The parameter D is obtained from β_2 by the relation

$$D = -\frac{2\pi c}{\lambda^2}\beta_2 \tag{II.6}$$

D generally used rather than β_2 and given in terms of λ rather than w. Rewriting II.4 for D in terms of λ we obtain [3]:

$$D(\lambda) = -\frac{\lambda}{c}\frac{d^2n(\lambda)}{d\lambda^2} = c\frac{dn_g(\lambda)}{d\lambda} \tag{II.7}$$

II.2.3 Effective mode area

The effective mode area (EMA) of fibers can be derived from the modal distribution $F(x,y)$ of the fundamental fiber mode and writes as

$$A_{eff} = \frac{\left(\iint_{-\infty}^{+\infty}|F(x,y)|^2 dxdy\right)^2}{\iint_{-\infty}^{+\infty}|F(x,y)|^4 dxdy} \tag{II.8}$$

Where $F(x,y)$ is the transverse distribution of the optical mode, for SMF the fundamental mode. The EMA of a fiber is important because nonlinear effects are rising with higher intensity density. Since PCFs often have small fiber cores, their EMA is small as well and nonlinear effects get more important. The other way around, large mode area fibers are especially made to avoid high nonlinear effects such as Brillouin and Raman Scattering. Later we will see that the EMA plays a role for the critical power for stimulated Brillouin scattering. [5]

II.2.4 Birefringence

The so called single mode fibers guide actually two optical modes simultaneously. They are orthogonally polarized and the two will propagate with the same velocity in perfectly radial symmetric fibers. In birefringent fibers, fibers that are not completely radial symmetric, these two modes have a different phase and group velocity because the refractive index is different for the different modes, propagating according to an x-axis and orthogonal y-axis. The phase modal birefringence is given by:

$$B_m = \frac{|\beta_x - \beta_y|}{k_0} = |n_x - n_y| = \Delta n \quad \text{(II.9)}$$

With β_i the mode propagation constant, k_0 the wave vector in vacuum and n_i the refractive index according to the axis. The group modal birefringence can then be written as:

$$\Delta N = \Delta n - \lambda \frac{d\Delta n}{d\lambda} \quad \text{(II.10)}$$

Conventional fibers are the oretically not birefringent but material and geometrical in homogeneities can induce a low birefringence in the order of 10^{-6}. As one may think that PCFs with a hexagonal structure may be birefringent since they have not the same air material distribution in x- and y-axis, it should be emphasized here, that this is not the case. The hexagonal symmetry of a perfect micro structured fiber leads to no, birefringence. Nevertheless, PCFs are more sensitive to irregularities, since small variations of the hole diameter lead to a different refractive index. Besides the drawing process of PCFs is more complicated and induces more fiber irregularities. On the other hand PCFs with asymmetrical air hole structure like two big air holes can reach ultra-high birefringence up to 10^{-2}. [5]

II.2.5 Losses mechanisms

II.2.5.1 Intrinsic loss

The optical loss α_{dB} ,measured in dB/km, of PCFs with a sufficiently reduced confinement loss can be expressed as:

$$\alpha_{dB} = A \backslash \lambda_4 + B + \alpha_{OH} - + \alpha_{IR} \quad \text{(II.11)}$$

Being A, B α_{OH}, and α_{IR} the Rayleigh scattering coefficient, the imperfection loss, and OH and infrared absorption losses, respectively. At the present time the losses in PCFs are dominated by OH-absorption loss and imperfection loss.

In a typical PCF the *OH* absorption loss is more than 10 dB/km at 1380nm and this causes an additional optical loss of 0.1 dB/km in the wavelength range around 1550 nm. Since this contribution is very similar to the intrinsic optical loss of 0.14 dB/km for pure silica glass at this wavelength, the *OH*-absorption loss reduction becomes an important and challenging problem.

Most of the *OH* impurities seem to penetrate the PCF core region during the fabrication process. As a consequence, a dehydration process is useful in reducing the *OH*- absorption loss.

Imperfection loss, caused mainly by air hole surface roughness, is another serious problem. In fact, during the fabrication process, the air hole surfaces can be affected by small scratches and contamination. If this surface roughness is comparable with the considered wavelength, it can significantly increase the scattering loss. Thus, it is necessary to improve the polishing and etching process, in order to reduce the optical loss caused by this roughness. Moreover, fluctuation in the fiber diameter during the fiber drawing process can cause an additional imperfection loss, if the air-hole size and pitch change along the fiber.

It is important to underline that the Rayleigh scattering coefficient of PCFs is the same as that of a conventional SMF. However, this is higher than that of a pure silica core fiber, although the PCF is made of pure silica glass. It is necessary to reduce the roughness further, in order to obtain a lower imperfection loss and a lower Rayleigh scattering coefficient. [1]

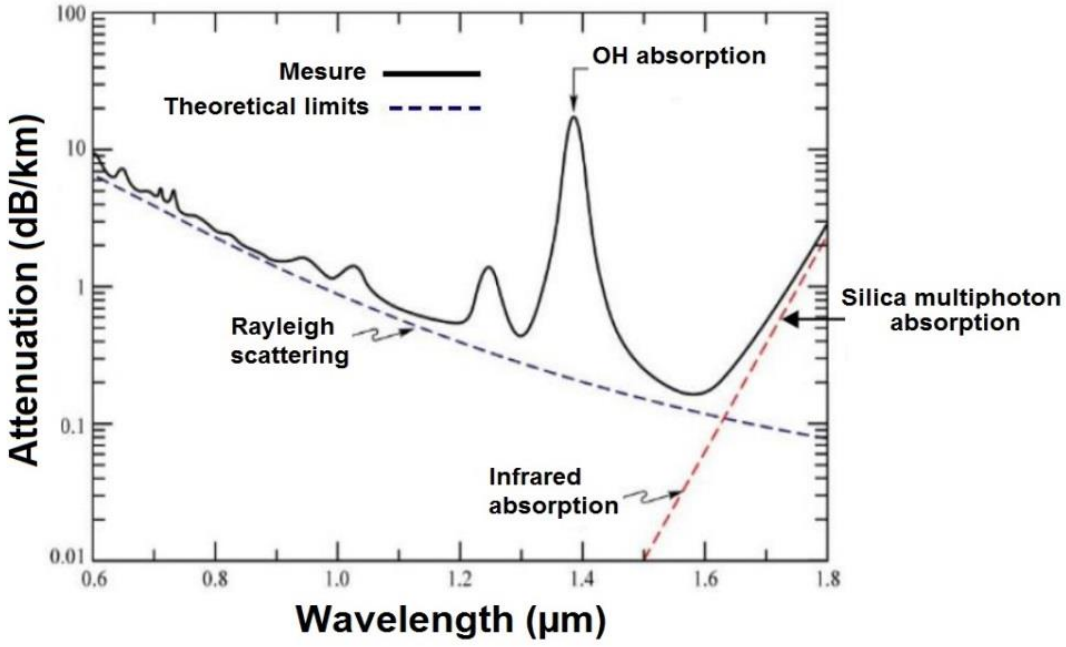

Fig II.3: Different sources of the attenuation in the silica fibers. [6]

II.2.5.2 Macro bending losses

The macro bending losses of optical fibers are very important to address, not only from a practical handling point of view, but also because they play a central role, when defining the spectral window, in which the fiber may be operated. The bending properties of PCFs were described by the introduction of a critical bend radius, a radius under which a PCF may not be bending in order for the excess bending loss to be below a given limit. The power loss coefficient due to macro bending is written as:

$$\alpha = \frac{\sqrt{\pi}A_e^2\rho.\exp(-\frac{4\Delta W^3}{3\rho V^2}\quad R)}{4PW\sqrt{\frac{WR}{\rho}+\frac{V^2}{2\Delta W}}} \qquad \text{(II.12)}$$

Where Δ is the relative index difference between the maximum refractive index in the core region and the cladding index ρ is the core radius, V is the normalized frequency, and W is the normalized decay parameter in the cladding. R de notes the radius of curvature, A_e is the amplitude coefficient of the cladding electric field, and P is the propagation power carried by the fundamental mode. Applying equation (II.12), the bend loss is directly calculated from the Bessel function coefficients and propagation constant of the effective index fiber. [7]

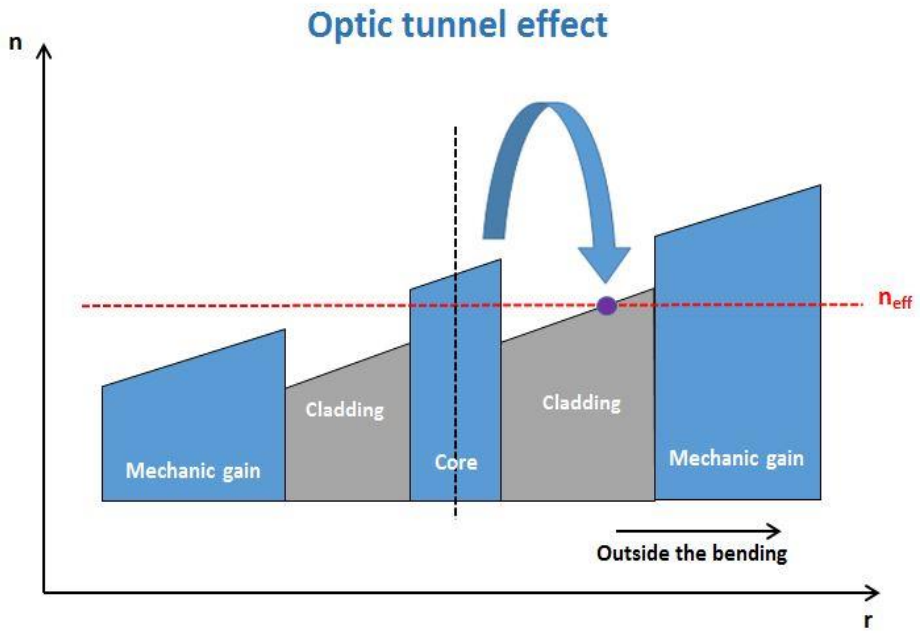

Fig II.4: Illustration of the optic tunnel effect in the standard fiber bending. The blue point in the cut off effective's index of fix λ recommend effective index equality between the core mode and the cladding mode modify by the bending. [8]

II.2.5.3 Confinement loss

The existence of layers of air holes in the PCF makes light leak out from the guiding region. The confinement loss is the fraction of leaky modes. The confinement loss is calculated from the imaginary part of the complex effective index [9]:

$$L_C = \frac{40\pi}{\ln(10)\lambda} Im(n_{eff}) \times 10^3 \, dB/km \qquad \text{(II.13)}$$

Where Im is the imaginary part of the n_{eff}

In PCFs, the matrix material of the core and the cladding is the same, so modes cannot be confined in the sense that they are in conventional (typically doped) fibers. Light is able to leak out or "escape" from the core both through the air holes and through the bridges between them. Loss through the air holes occurs because the holes are relatively small, allowing an evanescent field to tunnel through them [see Fig II.5 (b)]. This process is equivalent to quantum mechanical tunneling, and also occurs in conventional fibers with a high index coating when the cladding is sufficiently thin. This kind of confinement loss applies to all modes, and its effect decreases exponentially with the number of rings of holes employed.

Light can also be lost through the high index bridges between the holes. This effect, by contrast, is very much stronger for high order modes than it is for lower order modes. As shown in Fig II.5, the microstructure can effectively act as a "sieve" confining modes which are spatially too large to pass through the bridges to a far greater extent than those with smaller lobes. The degree of confinement loss can vary over several orders of magnitude for different modes.

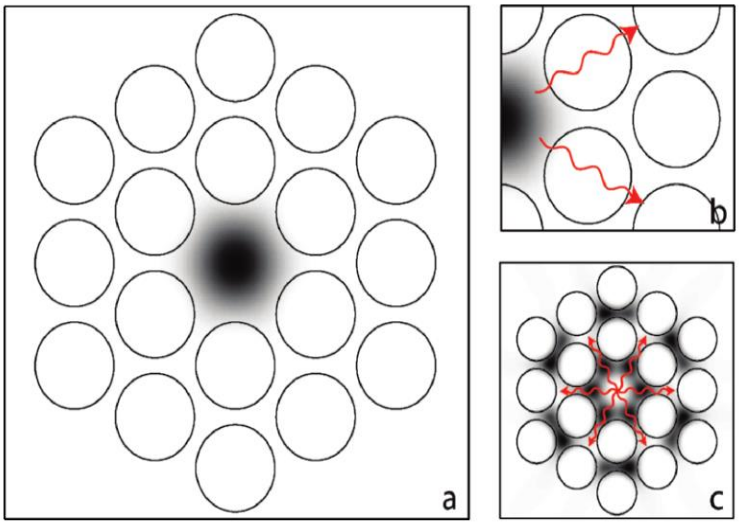

Fig II.5: The fundamental mode in a MOF is well confined by the hole structure (a), though some light tunnels through the air holes (b), and through the bridges between the holes (c). The latter process strongly affects the confinement of higher order modes whose smaller features are less confined by the hole structure. [2]

Confinement loss in a microstructured cladding is a property that cannot be properly understood using a naive "homogenized" description. In single mode fibers and bandgap fibers, its impact is mostly felt in terms of defining the air fraction or number of rings of holes that are required to reduce loss to the desired levels. In multimode fibers, it is particularly significant as the large differential mode attenuation effectively defines the modes that propagate down the fiber.

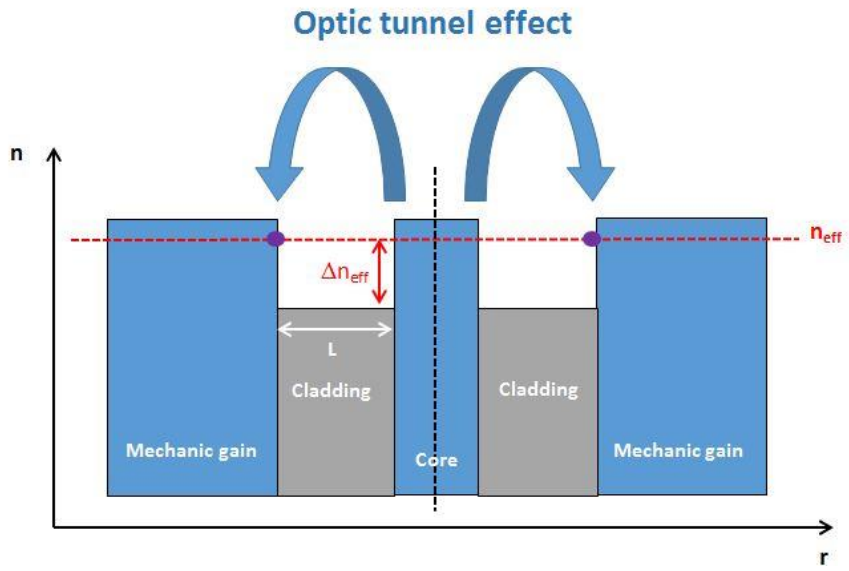

Fig II.6: Illustration of the optic tunnel effect in the sault index law fiber. The blues points in the cut off effective's index of fix λ recommend effective index equality between the core mode and the cladding mode. [8]

II.3 Modeling methods

Commonly used methods for modeling of optical fibers cannot be applied successfully in PCF modeling. These fibers have a high refractive index contrast and a sub wavelength periodical structure. Therefore, the methods used in modeling photonic crystals and electromagnetic fields are adapted to this purpose.

II.3.1 Beam propagation method (BPM)

This approach was not initially intended to find modes but rather to simulate propagation along non uniform waveguides, tapers and couplers. The structure is divided into thin discrete layers transverse to the direction of propagation; then the effects of diffraction and refraction are alternately considered. Diffraction can be modeled either by finite differences or Fourier transform techniques leading to a diversity of beam propagation methods.

This is a computationally intensive approach, which is probably more suited to non-uniform structures. This method has been used to study the higher order guided modes and so called inner cladding modes in a fiber with a ring of six large air-holes surrounding a doped core. [2]

II.3.2 The full vector plane wave expansion method (PWE)

The full vector plane wave expansion (PWE) method offers a very efficient and straightforward approach to model PCFs. This method allows solving the full vector wave equation for the magnetic field. In this model a periodic field as well as a position dependent dielectric constant is represented using Fourier expansion in terms of harmonic functions defined by the reciprocal lattice vector.

From Maxwell's equations the full-vector wave equation is obtained for magnetic field H_k:

$$\nabla \times \left[\frac{1}{\varepsilon(r)}\nabla \times H_k\right] = -\frac{w^2}{c^2}H_k \qquad \text{(II.14)}$$

Where k is the wave vector and $\varepsilon_{(r)}$ is a value of the dielectric constant in the structure. A simulated PCF structure is represented as a periodic super cell, which contains a crystal structure and its defects. Due to the periodicity we can express H_k as a sum of plane waves based on Bloch theorem:

$$H_k = \sum_G h_k - G \exp(-i(k-G).r) \qquad \text{(II.15)}$$

Where G is a lattice vector in reciprocal space. The dielectric constant $\varepsilon(r)$ is represented with a Fourier expansion:

$$\frac{1}{\varepsilon(r)} = \sum_G V\, exp(iG.r) \qquad \text{(II.16)}$$

Where

$$V_G = \frac{1}{A_u}\int \frac{1}{\varepsilon(r)} exp(-iG.r)\, dr \qquad \text{(II.17)}$$

And A_u is the area of a unit cell.

The PWE allows calculating dispersion relations and photonic bandgap in periodic dielectric structures (Fig II.7).

It can be applied to any type of crystal structure, including irregular crystals. It allows finding photonic band structure in the PBG guidance mechanism, as well as modes in the effective index guidance mechanism. It is an accurate, relatively fast method, however it has several drawbacks. It cannot be used for calculating structures with active materials (absorption and amplification). Also, it does not bring any information about scattering losses, transmission and reflection of incident light in the PCF. [10]

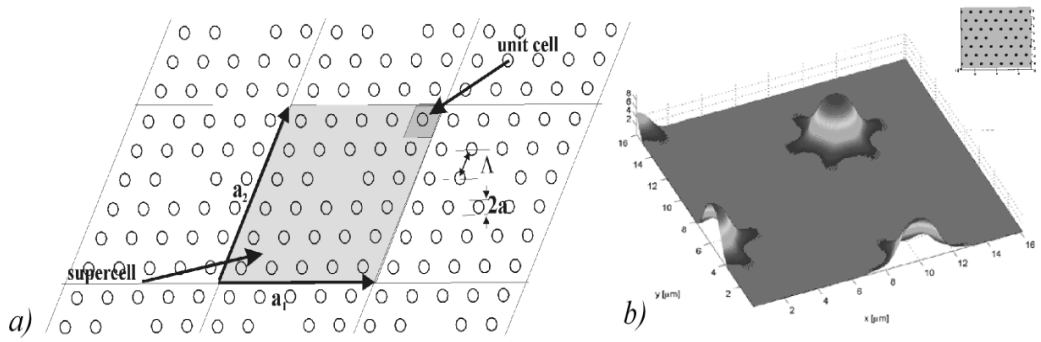

Fig II.7: PWE simulation: (a) the PCF structure is represented as a periodic supercell, which contains crystal structure and its defects; (b) an example of simulation results with PWE — intensity distribution in periodic supercells. [10]

II.3.3 Localized basis functions method (LBF)

The method of localized basis functions (LBF) is based on direct solution of Maxwell's equations, similarly to the PWE method. It assumes that guided modes of PCF are localized in the close area around the crystal defect and the modes can be described as a sum of Hermite Gaussian functions localized in the neighborhood of the core. It allows reducing dramatically the number of base functions and computational complexity. In the LBF method a medium transnationally invariant along z the axis is assumed and Maxwell's equations are written as wave equations for transversal magnetic field:

$$(\nabla_\perp^2 + k^2\varepsilon)h_\perp + (\nabla_\perp \ln(\varepsilon)) \times (\nabla_\perp + h_\perp) = \beta^2 h_\perp \qquad \text{(II.18)}$$

Where $\nabla_\perp$ is the gradient in the transversal plane and $h_\perp$ are transversal components of the magnetic field $H_{i,i} = x, y$:

$$H_i = h_i \exp(i(\beta z - ckt)) \qquad \text{(II.19)}$$

Base functions are built of the set of Hermite- Gaussian functions:

$$\phi_{mn} = \exp(-\frac{x^2+y^2}{2\Lambda^2})H_m\left(\frac{x}{\Lambda}\right)H_n\left(\frac{y}{\Lambda}\right) \quad \text{(II.20)}$$

Where H_m is the Hermite polynomial of the order m. The functions ϕ_{mn} are orthogonal and create a complete system of the base. The wave equation (II.18) can be noted in the following algebraic form:

$$\sum_{k,l} L_{k,l}^{m,n} h_{\perp}^{k,l} = \beta^2 h_{\perp}^{m,n} \quad \text{(II.21)}$$

Where $L_{k,l}^{m,n}$ are the matrix coefficients of the left-hand side operator in (II.18) and $h_{\perp}^{k,l}$ is the transversal magnetic field in Hermite- Gaussian basis. Solving eigenvalue problem propagation constant β and field distribution can be obtained. This method has been developed for modeling PCF with circular holes and hexagonal lattice. It allows modeling of modal and dispersion properties of the PCFs.

The supercell lattice method is a combination of PWE and LBF methods. The electric field is decomposed by use of Hermite - Gaussian functions. PCF is decomposed on two virtual different periodic dielectric structures of perfect photonic crystals. The first one represents a photonic crystal of photonic cladding, while the second photonic crystal represents central defects of the PCFs. The structures of both virtual PCs are expanded in cosine functions. From the wave equation and the orthonormality of the Hermite- Gaussian functions, the propagation characteristics of the PCFs, such as the mode field distribution, the effective area, and the dispersion property, is obtained. [10]

II.3.4 The full-vector finite element method (FEM)

The full-vector finite element method (FEM) has been applied to PCF modeling successfully. It allows calculating both dispersion and confinement properties of PBG and solid core structures. For a given frequency the method provides us with a complex propagation constant $\gamma(w) = \beta(w) + i\alpha(w)$ where β is the standard propagation constant of the plane-wave along the fiber and $\alpha$is the attenuation constant associated with the exponential decay along the fiber axis. [10]

II.3.5 A multipole method (MPM)

A multipole method originally developed for modeling diffractive structures and photonic crystals has been successfully used for index and photonic bandgap guiding PCFs.

In this method the field is written in terms of cylindrical harmonics centered around each air hole. The method has advantages in terms of speed and accuracy. Since finite cladding is assumed, the calculations can be performed in this way.

Apart from the above-mentioned methods there are several other ones used for PCF modeling: scattered matrix method, transferred matrix method and others. However mostly used are PWE, FD, and multipole methods for modeling properties of PCFs. [10]

II.3.6 The finite difference time domain method (FDTD)

The finite difference time domain (FDTD) method is widely used for calculation of the evaluation of an electromagnetic field in depressive media. The wave propagation through the PCF structure is found by direct integration in the time domain of Maxwell's equations in a discrete form. Space and time is discrete in a regular grid. Evaluation of the electrical and magnetic field is calculated on a Yee cell (Fig II.8). In addition the boundary conditions are added (absorbing or periodic ones). Most often uniaxial perfect matching layer (UPML) boundary conditions are used for PCF modeling. The method allows obtaining transmission and reflection coefficients, energy flow of propagation fields (Poynting as well as the temporary field distribution).

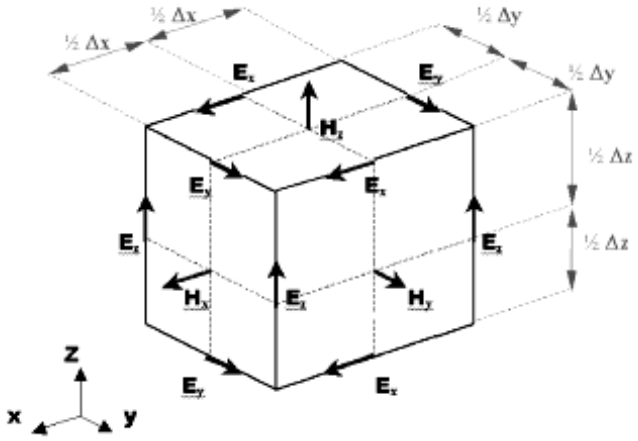

Fig II.8: The Yee cell describes all components of electrical and magnetic field in a cube. Every component of the electromagnetic field is defined only in one place in the unit Yee cell. [10]

The FDTD method is universal, robust, and methodologically simple. The main drawback of this method is very high time and memory complexity of the algorithm. Since PCF are 3D structures with 2D refractive index distribution only short pieces of the fiber can be simulated with these methods. It can be successfully applied to model tapers, couplers, and double core coupling in the PCFs.

Large volume simulations can be performed with computer clusters because the FDTD method can be relatively easily implemented as a parallel algorithm.

Similar discretization schemes can be used in the context of the beam propagation method (BPM) or finite difference (FD) mode solvers. Zhu et al. use the 2D Yee discretization scheme in their full vector finite difference mode solver to express transversal electrical and magnetic field discrete form. By applying the finite difference procedure, the full vectorial wave equation yields the algebraic eigenproblem. [10]

II.3.7 The finite difference frequency domain method (FDFD)

In the finite difference frequency domain (FDFD) mode solvers, two discretization schemes have been used by Zhu *et al.* One is that first proposed by Stem, in which possible discontinuities lie between two adjacent mesh grids and every grid point corresponds to a unique refractive index. The wave equation in terms of transverse electric field E_t, (or magnetic field H_t) may be expressed as follows:

$$(\nabla_t^2 + k_0^2\varepsilon_r)\overline{E_t} + \nabla(\varepsilon_r^{-1}\nabla_t\varepsilon_r.\overline{E_t}) = \beta^2\overline{E_t} \qquad \text{(II.22)}$$

Or

$$(\nabla_t^2 + k_0^2\varepsilon_r)\overline{H_t} + \varepsilon_r^{-1}\nabla_t\varepsilon_r \times (\nabla_t \times \overline{H_t}) = \beta^2\overline{H_t} \qquad \text{(II.23)}$$

Where $k_0 = 2\pi / \lambda$ the wave number in free space is, ε_r is the waveguide dielectric constant, and β is the propagation constant. These equations are directly discretized by finite difference as presented in. This discretization scheme is usually used in the context of the beam propagation method (BPM), another discretization scheme is that first proposed by Bierwirth et al... In this second scheme, possible discontinuities lie on the mesh grids, so that any grid point can be associated with up to four different refractive indices. The transverse magnetic components are usually used in deriving the discretization matrix.

In Yee's mesh, the mesh grids for electric fields lie on possible dielectric discontinuities. Since all the transverse field components are tangential to the unit cell boundaries, the continuity conditions are automatically satisfied. Zhu et al. assumes that the fields have a dependence of position z and time t according to $exp[j(-\beta z + wt)]$.

From Maxwell's curl equations ($\nabla \times \bar{E} = -\partial \bar{B}/\partial t$, $\nabla \times \bar{H} = -\partial \bar{D}/\partial t$) after scaling $\bar{E}$by the free-space impedance $Z_0 = \sqrt{\mu_0/\varepsilon_0}$, we then have [7]:

$$jk_0 H_x = -\partial E_z/dy + j\beta E_y \quad \text{(II.24)}$$

$$jk_0 H_y = \partial E_z/dx + j\beta E_x \quad \text{(II.25)}$$

$$jk_0 H_z = -\partial E_y/dx + \partial E_x/dy \quad \text{(II.26)}$$

and

$$jk_0 \varepsilon_r E_x = \partial H_z/dy + j\beta H_y \quad \text{(II.27)}$$

$$jk_0 \varepsilon_r E_y = -\partial H_z/dx - j\beta H_x \quad \text{(II.28)}$$

$$jk_0 \varepsilon_r E_z = \partial H_y/dx - \partial H_x/dy \quad \text{(II.29)}$$

Equations (II.24-II.29) are now discretized, and Zhu et al. obtains the following type of equations:

$$jk_0 H_x(i,j) = -[E_z(i,j+1) - E_z(i,j)]/\Delta y + j\beta E_y(i,j) \quad \text{(II.30)}$$

$$jk_0 H_y(i,j) = j\beta E_x(i,j) + [E_z(i+1,j) - E_z(i,j)]/\Delta x \quad \text{(II.31)}$$

$$jk_0 H_z(i,j) = -\left[E_y(i+1,j) - E_y(i,j)\right]/\Delta x + [E_x(i,j+1) - E_x(i,j)]/\Delta y \quad \text{(II.32)}$$

The equations (II.27-II.29) may be written in a similar manner. We note that the terms j in the brackets indicate a number (and this number has nothing to do with the complex term appearing outside the brackets). Note, furthermore, that Zhu et al. approximate the refractive indices by averaging the refractive indices of adjacent cells. [8]

The equations (II.30-II.32), and the corresponding discretized equations representing the equations (II.27-II.29), can be written in matrix form as follows:

$$-jk_0\begin{bmatrix}\overline{H_x}\\ \overline{H_y}\\ \overline{H_z}\end{bmatrix}=\begin{bmatrix}0 & jB\bar{I} & \overline{U_y}\\ -jB\bar{I} & 0 & -\overline{U_x}\\ -\overline{U_y} & \overline{U_x} & 0\end{bmatrix}\begin{bmatrix}\overline{E_x}\\ \overline{E_y}\\ \overline{E_z}\end{bmatrix} \tag{II.33}$$

$$-jk_0\begin{bmatrix}\varepsilon_{rx} & 0 & 0\\ 0 & \varepsilon_{ry} & 0\\ 0 & 0 & \varepsilon_{rz}\end{bmatrix}\begin{bmatrix}\overline{E_x}\\ \overline{E_y}\\ \overline{E_z}\end{bmatrix}=\begin{bmatrix}0 & jB\bar{I} & \overline{V_y}\\ -jB\bar{I} & 0 & -\overline{V_x}\\ -\overline{V_y} & \overline{V_x} & 0\end{bmatrix}\begin{bmatrix}\overline{H_x}\\ \overline{H_y}\\ \overline{H_z}\end{bmatrix} \tag{II.34}$$

Where $\bar{I}$ is a square identity matrix, and $\varepsilon_{rx}, \varepsilon_{ry}\ and\ \varepsilon_{rz}$ are diagonal matrices determined by the following equations:

$$\varepsilon_{rx}(i,j) = [\varepsilon_r(i,j) + \varepsilon_r(i,j-1)] / 2 \tag{II.35}$$

$$\varepsilon_{ry}(i,j) = [\varepsilon_r(i,j) + \varepsilon_r(i-1,j)] / 2 \tag{II.36}$$

$$\varepsilon_{rz}(i,j) = [\varepsilon_r(i,j) + \varepsilon_r(i-1,j-1) + \varepsilon_r(i,j-1) + \varepsilon_r(i-1,j)] / 4 \tag{II.37}$$

In Eqns. (II.33- II.34), the matrices $\overline{U_x}, \overline{U_y}, \overline{V_x}\ and\ \overline{V_y}$ are square matrices, which depend on the boundary conditions of the rectangular computation window. Now having established a set of matrix equations including the finite difference formulation, these may be solved using available numerical eigenvalue routines, which then provide the effective modal index $n_{eff} = \beta / k_0$ and modal fields of the guided modes.

In the finite difference analysis of waveguides with curved interfaces, the staircase approximation has to be used in the rectangular mesh. In order to improve this approximation, Zhu et al. Use averaged refractive indices for the mesh cells across the interface. Similar techniques have been previously used in the plane wave expansion method and FDTD analysis. The use of the averaged refractive index of interfacial cells can significantly accelerate convergence and improve the modeling accuracy for waveguides with curved interfaces, such as PCFs. [7]

II.4 Conclusion

In this chapter, we have regarding the operational principle, the high index core PCFs, therefore, are comparable to conventional fibers. These PCFs do, however, display a number of properties that separate them significantly from conventional fibers. And different numerical methods, which over the past 7 years have been developed for the analysis and design of photonic crystal fibers. Some of the methods are fundamentally interesting for the understanding of the development of the required waveguide theory whereas others are of a more general character, and they have not been discussed in much detail here. Yet other methods have their strength in a relative simple formulation, although the same methods generally are insufficient for accurate parameter determination for calculation on band gap fibers.

In Table II.1, we present the advantages and disadvantages associated with each method

Method	***Advantages***	***Disadvantages***
Beam Propagation Method (BPM)	Reliable (well tested) method Commercially available May use complex prop constant	Relatively computationally inefficient
Finite Difference Methods (FDTD , FDFD)	Very general approach May describe arbitrary structures Well established and tested	Non—modal approach Numerically intensive Requires detailed treatment of boundaries
Plane Wave Expansion Method (PWE)	Well suited for PBGs Good agreement with experiments demonstrated Widespread approach	Large supercells needed for complex structures Very demanding for full fiber analysis
Localized Basis Functions Method (LBF)	Solutions may be adapted to finite size structures May describe random hole distributions	Needs great care on result interpretation Rel, complex method Inefficient PBG analysis
Finite Element Method (FEM)	Reliable (well tested) method Accurate modal descript	Complex definition of calculation mesh
Multipole method (MPM)	Describes effects of finite cladding region No false birefringence errors Suited for symmetry stud Leakage loss prediction	Cannot analyses arbitrary cladding configurations

Tab II.1: Overview of advantages and disadvantages concerning different numerical methods used for analysis and design of photonic crystal fibers. [8]

References

[1] Federica Poli, AnnamariaCucinotta, Stefano Selleri, Photonic *crystal fibers: properties and applications, Springer (2007).*

[2] Maryanne C. J. Large, Leon Poladian, Geoff W. Barton, Martijn A. van Eijkelenborg (auth.), *Microstructured Polymer Optical Fibres,* Springer US (2008)

[3] James Morgan Stone , *PHOTONIC CRYSTAL FIBRES AND THEIR APPLICATIONS IN THE NONLINEAR REGIME* ,PhD thesis , University of Bath , April 2009

[4] DAOUI Abdel Kader , *Fibres optiques microstructurées : Modélisation et optimisation des propriétés optiques*, MAGISTER thesis , BADJI MOKHTAR-ANNABA UNIVERSITY ,2009

[5] Birgit Stiller , *Brillouin scattering in photonic crystal fiber: from fundamentals to fiber optic sensors, PhD thesis* , University of Franche-Comté ,2011

[6] IreneBroquet, "*La diffusion dans les fibres optiques multimodes*", Annales de télécommunications, 29, 195-208, (1974).

[7] Anders Bjarklev, JesBroeng, Araceli Sanchez Bjarklev (auth.), *Photonic Crystal Fibres, Springer US (2003).*

[8] Aurélie Bétourné, "*Conception et caractérisation de nouvelles fibres optiques a cristal photonique dites hybrides et applications a l'optique non linéaire*", Thèse de doctorat, Lille 1 University, (2010).

[9] I. Abdelaziz, F. AbdelMalek, H. Ademgil, S. Haxha, T. Gorman, and H. Bouchriha , *Enhanced Effective Area Photonic Crystal Fiber With Novel Air Hole Design* , JOURNAL OF LIGHTWAVE TECHNOLOGY, VOL. 28, NO. 19, OCTOBER 1, 2010

[10] R. Buczynski , *Photonic Crystal Fibers ,Proceedings of the XXXIII International School of Semiconducting Co mpounds*, Jaszowiec 2004

Chapter III

Modeling results of ZBLAN PCF by the finite difference frequency domain method

III.1 Introduction

Silica optical fiber is used to transmit light and information over long distances in optical communication from O to U band. Current optical communication focuses on 1.55 μm wavelength due to fused silica material having the lowest intrinsic material attenuation loss of 0.185 dB/km at this particular wavelength. Further reduction of the intrinsic loss for fused silica is impossible. Therefore, replacing the optical fiber with material that has a lower intrinsic material loss is an alternative method to reduce the attenuation loss and increase transmission distance in optical communication that is ZBLAN material. [1]

Using the Lumerical application , we numerically study the fundamental characteristics of ZBLAN CL-PCF for possible optical communication within 0.5 μm to 1.8 μm ,we'll present the numerical results obtained by the FDFD method for large effective area PCF with a circular structure, then we'll present the structure used and their opto-geometrical parameter, after that we'll expose the result obtained by the simulation for the different optical proprieties of this structure, Finally, we completed our study with an analysis of the generation supercontinuum for 1.55 μm in our optimized PCF and a review of its most used application.

III.2 ZBLAN photonic crystal fiber

III.2.1 ZBLAN material

Among the existing non-silica glasses, zirconium fluoride-based (ZrF4 > 50 mol %) ZBLAN (ZrF4–BaF2–LaF3–AlF3–NaF) glass is transparent from 0.2 to 7.8 μm and has been viewed as an attractive material for optical devices from the deep-ultraviolet to the mid-infrared. Since its discovery in 1975, ZBLAN has been regarded as a promising replacement for fused silica in telecommunications, suggesting that data transmission could be shifted to longer wavelengths where its attenuation is intrinsically much lower (less than 0.01 dB km–1 at 2.5 μm) than in fused silica (0.185 dB km–1 at 1.55 μm).[2]

III.2.2 Structure and opto-geometrics parameters

The transversal section of large effective area CL-PCF is presented in Fig III.1; the cladding contains five crowns of air holes arranged with a circular structure. The solid core is obtained by the elimination of air holes in the center of the structure, the first crown of air holes near the center is injected with different values of refractive index (different liquids).The material which is ZBLAN and its refractive index is modeled according to the formula Sellmeier, the diameter of the air holes near the center, the diameter of the other air holes and the pitch are, respectively, d_1, $d_2$and Λ.

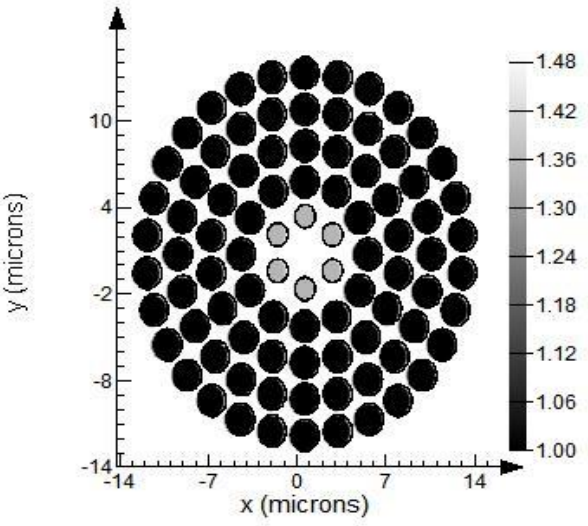

Fig III.1 : Structure of the large effective area CL- PCF with Λ=2.5μm, d_1=1.4 μm, d_2=2.2 μm.

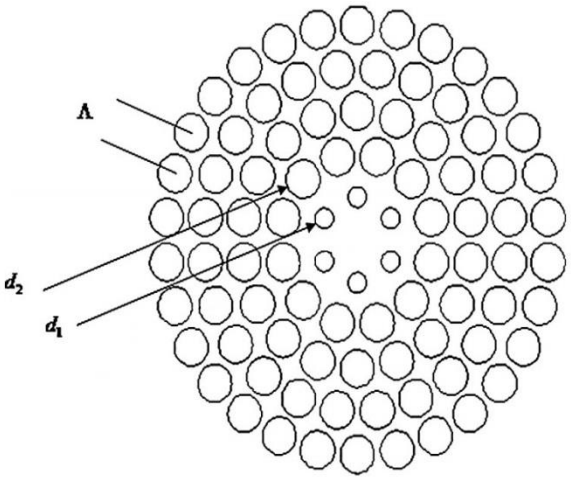

Fig III.2 : Cross sectional view of the PCF, showing the opto-geometrical properties.

Fiber optic large effective areas are used to transport light beams of high optical power with a minimum of non-linear effects and without damaging the medium of propagation. They are used in several applications such as fiber lasers [3], fiber amplifiers [4], multiplexed telecommunications systems Wavelength Division

Multiplexing (WDM) [5] and home distribution networks (Fiber To The Home: FTTH).[6]

Choosing the number of crowns (five) is done to ensure a good confinement of the light in the core also the diameter of the air holes d_1 and d_2,in the figure below shown that the light is confinement in the center of the structure.

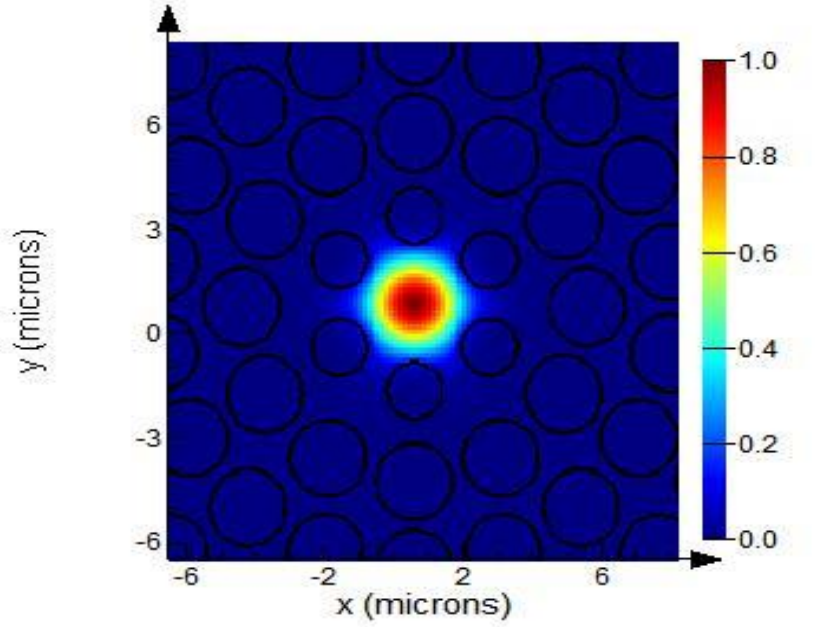

Fig III.3 : The optical field distribution of the fundamental mode of PCF with Λ = 2.5 µm, d_1= 1.4µmand d_2= 2.2µm for the wavelengths 1.55µm.

III.3 Simulation results

We'll use the FDFD method in order to obtain the chromatic dispersion, confinement losses, effective mode area that we can calculate with the equation II.7, II.13, II.8 and non-linearity.

III.3.1 Chromatic dispersion

The Fig III.4 present the evolution of the chromatic dispersion according to the wavelength, and we'll use two different diameters (d_1=1.4µm and d_2=2.2µm in Fig III.4.a) and (d_1=1.6µm and d_2=2.2µm in Fig III.4.b), the pitch is 2.5µm within wavelength from 0,5 µm to 1,8 µm , in order to see the effect of changing the opto-geometrical properties (d_1,d_2, Λ)of the fiber on the chromatic dispersion .

The first crown of air holes near the center (d_1) is injected with different fluids with various refractive indexes (n_{eff}), methanol (n_{eff} = 1.33), propane (n_{eff}= 1.34), ether (n_{eff}= 1.35),ethanol (n_{eff}= 1.36), hexane (n_{eff}= 1.37). [7]

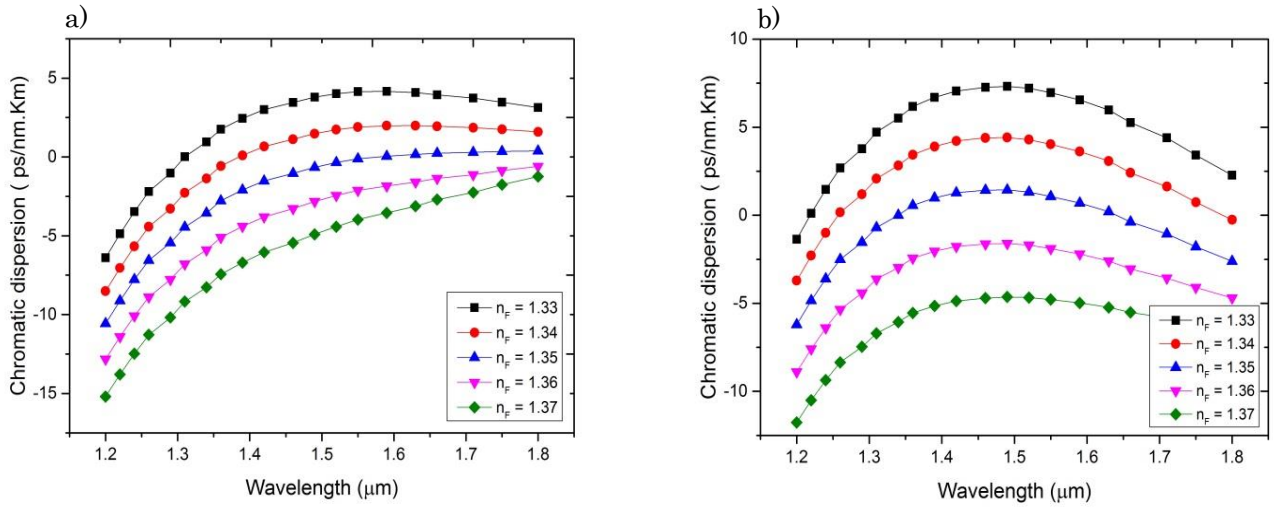

Fig III.4 : The evolution of the chromatic dispersion according to the wavelength, using two different diameters (d_1=1.4μm and d_2=2.2μm, Fig.III.4.a) and (d_1=1.6μm and d_2=2.2μm, Fig III.4.b), the pitch is 2.5μm, with different refractive index.

The aim of our studies is to obtain nearly zero ultra-flattened chromatic dispersion, we are interest in telecommunication domain within wavelength is 1.55 μm, we notice that from all the refractive index 1.35 is the best for both cases 1.4μm and 1.6μm, for 1.4μm the value of the chromatic dispersion is -0.114 ps/nm.Km for λ=1.55 μm and for 1.6 μm the value of the chromatic dispersion is 1.061 ps/nm.Km for λ=1.55 μm.

III.3.1.1 Chromatic dispersion optimization

The chromatic dispersion optimization in an optical fiber has a huge importance in lots of application such as supercontinuum generation or the interferometry in white light. One of PCFs advantages is easiness to control their optical proprieties therefore adjust their opto-geometrical parameters.

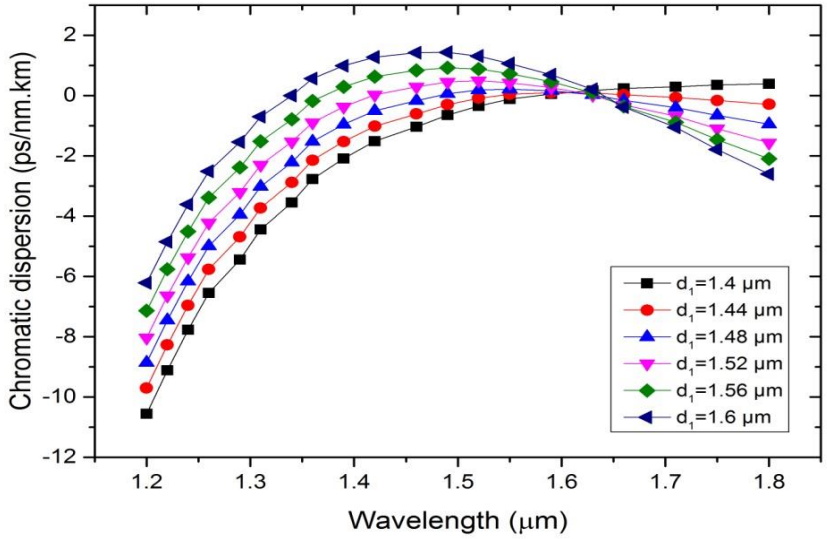

Fig III.5 : Large variationof chromatic dispersion from d_1= 1.4 μm to 1.6μm with a 0.04 μm step function to wavelength.

In the precedent results, we notice that from all the refractive index 1.35 is the best for both cases 1.4µm and 1.6µm, as a result we are going to calculate chromatic dispersion for a wavelength from 1,2µm to 1,8 µm with Λ =2,5 µm , by changing the diameter d_1 from 1,4 µm to 1,6 µm and with a step 0,04 µm .

The purpose of our study is to obtain a fiber with a flattened chromatic dispersion , so after we calculated the chromatic dispersion for a large variation shown in Fig III.5 , we notice that the chromatic dispersion increase with the raise of the diameter d_1 , like we said we are in telecommunication domain so the value of the chromatic dispersion for d_1=1.4 µm is -0.114 ps.nm/km, d_1=1.44 µm is 0.040 ps.nm/km , d_1=1.48 µm is 0.215ps.nm/km , d_1=1.52 µm is 0.424 ps.nm/km , d_1=1.56 µm is 0.723 ps.nm/km and d_1 =1.6 µm is 1.061 ps.nm/km , from all those different values we notice that d_1=1.4µm and d_1=1.44 µm gives us a chromatic dispersion nearly to zero , from the graph we notice that d_1=1.4 µm is nearly flattened to the zero , this large variation proves what we did in last study of the chromatic dispersion , that the changing of the opto-geometrical parameter effects the optical properties.

III.3.2 Confinement loss

In order to have a good light confinement in the core of the fiber, a lot of opto-geometrical are concerns (diameter, the pitch), in our case we'll be changing the diameter d_1 and see the effect of that variation the analyze of the confinement loss is done for Λ=2.5 µm with changing the diameter d_1 from 1.4 µm to 1.6 µm with step 0.04 µm, the result shown in figure below.

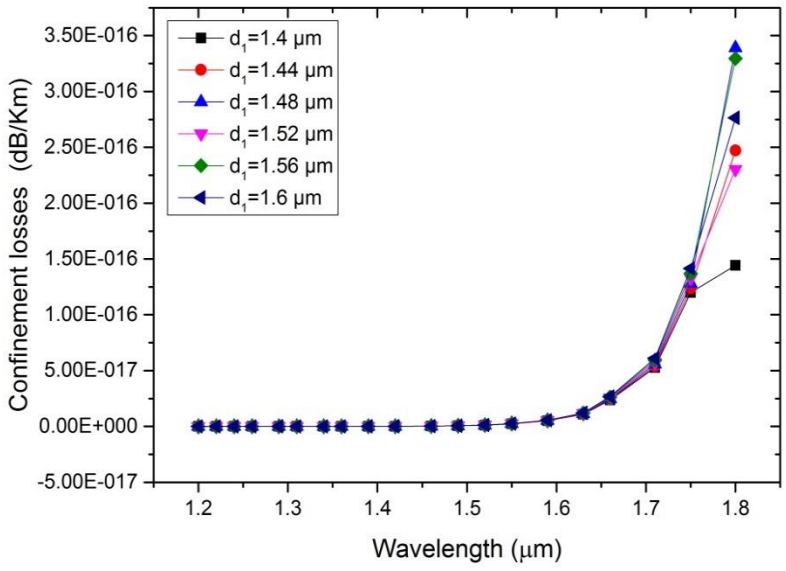

Fig III.6 : Evolution of confinement losses according to the wavelength for different diameter values.

From the Fig III.6 we notice that the more we increase the diameter d_1(therefor proportion of air in the cladding) the loss increases, also the loss increases respectively with wavelength, the value of the losses in λ=1.55µm for d_1=1.4µm is $2.3647.10^{-18}$dB/km , d_1=1.44 µm is $2.4158.10^{-18}$dB/km, d_1=1.48µm is $2.48866.10^{-18}$dB/km, d_1=1.52 µm is $2.55172.10^{-18}$ dB/km, d_1=1.56 µm is $2.54259.10^{-18}$dB/km and d_1= 1.6 µm is $2.55781.10^{-18}$ dB/km, from those previous results we can notice that d_1=1.4 µm give us a minimum loss compare to the other diameter .

III.3.3 Effective mode area

We have calculated the effective with Eq II.8 and the results are presented in figure below, effective area is an important parameter for a lot's of application (such as WDM, FTTH...etc.).

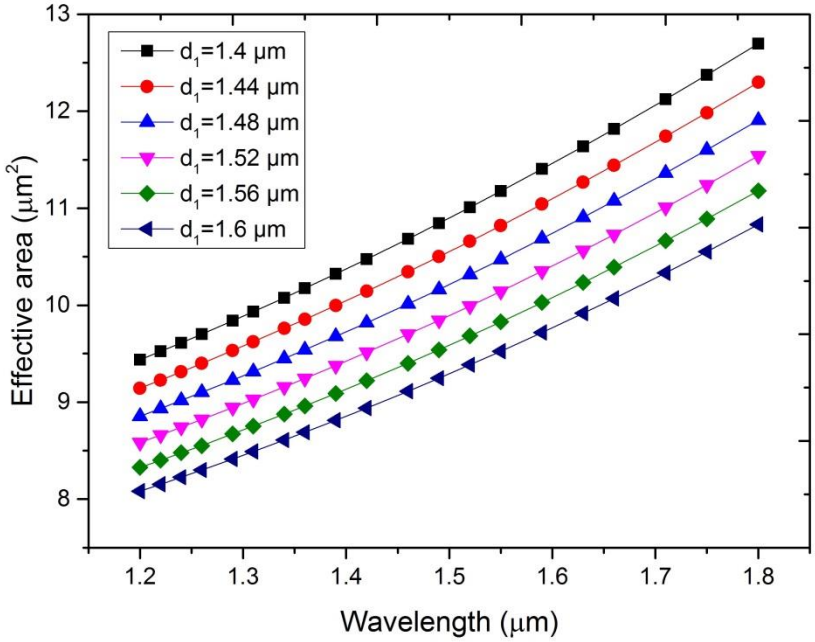

Fig III.7 : Evolution of the effective mode area in function to wavelength with Λ =2, 5 µm, with d_1 changing from 1.4 µm to 1.6 µm by 0.04 µm step.

We have increase the diameter d_1 from 1.4µm to 1.6µm and see the effect of changing the opto-geometrical parameter on the effective area, we notice that the more the diameter increases the more the effective area decreases and that's because when we increases the diameter of d_1 the region of the core decreases respectively.

From the Fig III.7 the diameter d_1=1.4 µm the one who provide the best result among the other diameter, we are interest in telecommunication domain so the value of the effective area in λ=1.55µm, for d_1=1.4 µm is 11.1766 (µm²).

III.3.4 Kerr Non linearity

Based on the effective mode area, we can obtain another important parameter for optical communication which is the nonlinearity of the fiber. The nonlinear coefficient is calculated with the following equation:

$$\gamma = \frac{2\pi}{\lambda}\frac{n_2}{A_{eff}}$$

Where n_2 is the material relate nonlinear Kerr coefficient and is equal to $5{,}4.10^{16}$ cm^2 W^{-1} for ZBLAN material [1].

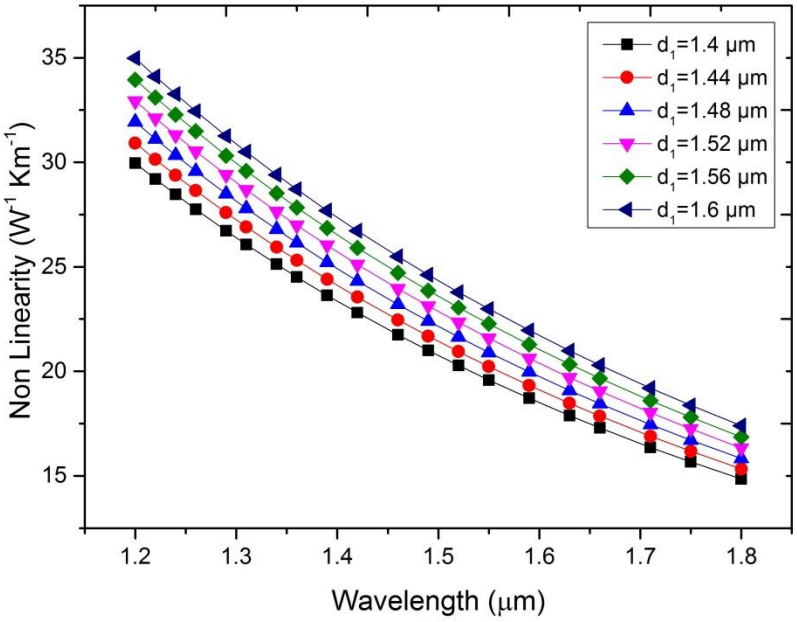

Fig III.8 : Evolution of Kerr non-linearity in function of the wavelength with variation of the diameter d_1 from 1.4 µm to 1.6 µm by step 0.04 µm.

Fig III.8 shows the nonlinear coefficient for ZBLAN PCF within the 1.2–1.8 µm wavelength region for various d_1 from 1.4 µm to 1.6 µm. Fiber with high nonlinearity favors the occurrence of nonlinear effects which will deteriorate the transmitted signal quality for optical communication. Therefore, for optical communication purposes, fiber with low nonlinearity is preferred. From our simulation, ZBLAN PCF with nonlinear coefficient is as 19.5854 W^{-1} km^{-1} at 1.55 µm wavelength when d_1=1.4 µm.

As we can see from the two graphs .The Figure III.8 and Figure III.7 are reversed as the region of the core with a radius of 1.4µm up to 1.6 µm have an coefficient of non-linearity very low , and the we notice that the more the wave increase the more the coefficient of non-linearity decreases .

III.4 Supercontinuum generation

The supercontinuum is a nonlinear optical phenomenon corresponding to the result of spectrum broadening of an optical wave during its propagation in an environment [8].The implementation of this phenomenon requires a nonlinear material with third-order susceptibility. It is important to highlight that the involvement of non-linear mechanisms in a supercontinuum regime depends on the time used as the excitation source and the geometrical and physical characteristics of the nonlinear medium [9]. However, these non-linear effects mainly occur a function of the applied light intensity thereof is modulated by the frequency of repetition and the time width of the pulses emitted by the source. This gives each temporal regime of the supercontinuum generation, a combination of nonlinear phenomena specific [2].

III.4.1 Supercontinuum generation in PCF

Supercontinuum generation in PCF In the late 90s, the PCF has attracted great interest for supercontinuum generation, due to their confinement capacity of light and the ability to change their dispersion by adjusting the geometry of the cladding. The first supercontinuum generated in PCF was noted experimentally in 2000.Ranka et al suffused pulses of 100 fs, energy of few nano-Joules, at 770 nm in a PCF of 75 cm length, designed so that its dispersion cancellation around 770 nm . They held a supercontinuum ranging from 400 to 1500 nm. Since then, several research works have emerged both experimentally and theoretically, with the understanding of the nonlinear effects involved in the supercontinuum generation in PCF and in regimes: femtosecond, nanosecond, and picosecond or quasi-continuous [10].

III.4.2 Application of Supercontinuum generation in telecommunications

Nonlinear propagation in optical fibers has been studied extensively in the context of optical telecommunications, and there has been much success in applications such as soliton transmission, Raman amplification and wavelength conversion (Agrawal2001) .The possible application of supercontinuum generation to telecommunications has also been a subject of intense research, where work has been particularly motivated by the need to develop broadband sources suitable for spectral slicing in wavelength-division multiplexing.

For such an application, a crucial practical requirement is spectral uniformity across as wide a wavelength range as possible around the 1550 nm telecommunications wavelength range. [11]

III.4.2.1 Pulse Compression and Short Pulse Generation

Ultra short optical pulses form the foundation of optical telecom systems. Information transmitted through telecom lines are encoded using amplitude and phase of such pulses. Therefore, it is essential for telecom to have reliable low-noise sources of high quality ultra-short laser pulses, especially broad band or multi-wavelength sources. The latter can be used for simultaneous transmission of many information channels through a single optical fiber, known as Wavelength Division Multiplexing (WDM)technology, which is the optical analogue of frequency division multiplexing commonly used for radio transmission.[12]

The fundamental limits on generation of few-cycle pulses by compression of SC spectra generated in microstructured fibers have been analyzed by Dudley and Coen (2004), confirming that quality of compressed pulses was closely related to spectral coherence of the SC. According to their work, a median coherence of about 0.7 could be expected to be a good benchmark for the potential compressibility of SC down to few-cycle pulses, provided compressors with sufficiently high resolution to compensate for the fine structure in the SC group delay were made available in the future. [12]

III.4.2.2 Pulse Train Generation at High Repetition Rates

Quite a simple and convenient technique for producing an ultra-short pulse train of high repetition rate was suggested by Hasegawa (1984) and for the first time was implemented by Tai et al. (1986) as early as 1986. This technique utilizes the effect of induced modulation instability, growth of initial relatively small intensity modulation amplitude of CW radiation due to modulation instability (MI). Such spectra sideband growth is an initial stage of spectral broadening and SC generation. [12]

III.4.2.3 Multi-wavelength Optical Sources

One of the most important applications of SC to the field of telecommunications is the design of multi-wavelength sources for ultra-broadband wavelength-division multiplexed (WDM) systems based on spectral slicing of SC generated by a sing le laser.

A powerful short optical pulse can be non-linearly broadened into a SC spectrum. This spectrum can then be sliced with an array of filters to create a series of WDM channels. This was the approach originally adopted by Morioka et al. (1993) using short (few ps) pulses with GHz repetition rates in dispersion-decreasing fiber (DDF) to create WDM pulsed sources.

SC WDM sources can be of great utility in more modest systems: Kartapoulosetal(2005), for example, studied the use of supercontinuum sources in coarse WDM applications with channel protection and concluded that in systems with a limited number of channels, the use of supercontinuum WDM sources can result in lower costs and increased reliability. [12]

III.4.2.4 Optical Fiber Characterization

Optical fiber plays crucial role in state of the art telecom industry. Besides standard SMF fibers, such as SMF -28, used for long-haul data transmission, there is a plethora of types of optical fibers used for amplification, dispersion compensation, optical processing, etc.

In order to improve existing legacy telecom system s, new types of fibers are constantly invented with tailored dispersion and non-linearity.SC provides a convenient, quick, and cost -effective way for characterization of optical fibers in a wide spectral range. Measurements of wavelength-dependent attenuation can be made simultaneously over a wide bandwidth, and group velocity- dispersion (GVD)measurements in conventional fiber with group delay resolutions of 0.01 ps/k m in fiber lengths of up to 130 km over more than 600 nm, using SC white pulses as was demonstrated by Mori et al. (1995).[12]

GVD measurements can also be carried out in non-typical media such as taperedair-silica microstructure fibers by means of white-light interferometry with the help of broadband sources, as demonstrated by Ye et al. (2002). Spectral interferometry with a SC source was also used by Jasapara et al. (2003) to perform GVD measurements in photonic bandgap fiber. González-Herráez et al.(2003) showed that continuous-wave generated SC could be effectively used to perform accurate, long-range (>200 km)measurements of polarization mode dispersion in fibers.[12]

III.4.2.5 Frequency Combs

One of the most fascinating applications of SC generation, which has revolutionized optical frequency metrology and may potentially have impact on telecom, is frequency comb generation.

An optical frequency comb is an optical spectrum showing spectral lines at fixed frequency spacing. A simple example would be the longitudinal mode structure at the output of a mode-locked cavity laser. By measuring frequency separation between laser radiation at a given frequency f and its second harmonic $2f$, the laser's absolute frequency can be determined .Hence, frequency combs can be used as "optical rulers" for high-precision spectroscopy and, by extension, for high- precision frequency or time-based metro logy, achieving accuracies of one part in 1017 in the measurement of optical clocks)Newbury, 2011; Ye and Cundiff, 2005).

In order for a frequency comb to be used for the purpose of determining absolute frequency, its spectrum must span at least a complete optical octave. The development of optical frequency combs earned Profs. John L. Hall and Theodor W. Hansch one half of the Nobel Prize in Physicsin 2005.[12]

III.4.3 Simulation results

Finally, we simulated the supercontinuum generation in the structure we have optimized; modeling supercontinuum generation is via solving the nonlinear Schrödinger equation [13]:

$$\frac{\partial A(z,t)}{\partial z}+\frac{\alpha}{2}A(z,t)+\sum_{k=0}^{\infty}\frac{i^{k-1}\beta_k}{k!}\frac{\partial^k A(z,t)}{\partial t^k}=i\gamma\left(1+\frac{i}{\omega}\frac{\partial}{\partial t}\right)\left(A(z,t)\int_{-\infty}^{\infty}R(t')|A(z,t-t')^2dt|\right) \quad \text{III.1}$$

In this equation $A(z,t)$ represents the temporal envelope of the pulse considered, z is the spatial variable in the propagation direction, α the loss coefficient, γ the nonlinear coefficient and $\beta_k=\frac{d^k\beta}{d\,\omega^k}$ the Taylor coefficients of the propagation constant β when developed in a Taylor series. These are responsible for the dispersion imposed on the pulses during propagation

The pulse propagating in PCF is modeled by a Gaussian function given by:

$$A(0,t)=\sqrt{P}\exp\left(\frac{-t^2}{2T_0}\right) \quad \text{III.2}$$

Where P = 3.2 kW is the peak power and T_0 = 100 fs is the pulse duration. Knowing the pumping wavelength is 1.55 µm; the resulting coefficients of the series development of Taylor β propagation constant are given by the following table:

Coefficient	Value
β2	-0.0043 ps^2/km
β3	-5.3659 $10^{-4} ps^3/km$
β4	3.1939 $10^{-6} ps^4/km$
β5	-1.5045 $10^{-8} ps^5/km$
β6	6.1302 $10^{-11} ps^6/km$
β7	-2.0171 $10^{-13} ps^7/km$
β8	4.8995 $10^{-16} ps^8/km$

Tab III.1 Coefficients of the series development of Taylor around 1.55 µm of propagation constant β.

In order to generate the supercontinuum we chose the fiber with nearly zero ultra-flattened chromatic dispersion, as we mention perversely the supercontinuum use in telecommunication domain, after we are done optimizing the fiber to obtain nearly zero ultra-flattened chromatic dispersion, we have acquired a fiber with achromatic dispersion 0.040 ps.nm/km for wavelength 1.55µm. the opto-geometrical properties of the optimized fiber (d_1=1.44µm, d_2=2.2µm and Λ = 2.5µm).

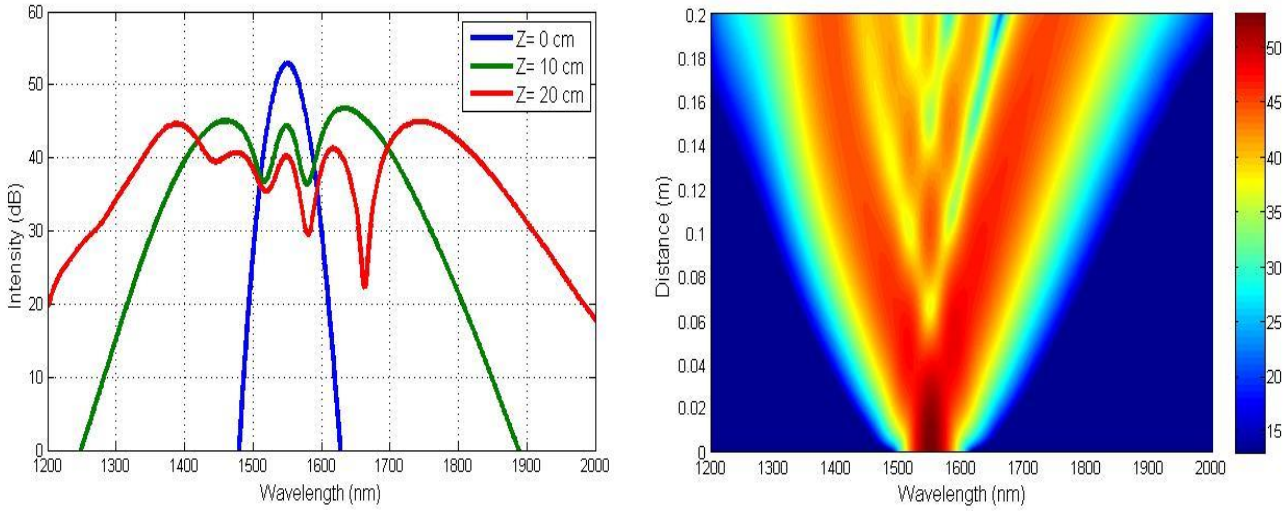

Fig III.9 : Evolution of the spectrum of a Gaussian pulse around 1.55 µm with temporal width of 100 fs in PCF of length 20 cm.

Fig. III.9 shows the evolution of the spectrum of the pulse as a function of the distance for a fiber length of 20 cm. Note that the spectrum of the pulse is widening with distance and reached 650 nm wide around the wavelength of 1.55 µm. The symmetrical

shape of the spectrum is achieved through the profile of virtually zero chromatic dispersion and ultra-flat on a wide range of wavelengths.

III.5 Conclusion

We have presented the numerical modeling on ZBLAN CL-PCF within 0.5–1.8μm wavelength for extremely low loss optical communication in mid-infrared region. We studied the fundamental characteristics of uniform circular lattice structure ZBLAN PCF such as chromatic dispersion, confinement loss, effective mode area, and kerr nonlinear coefficient, which served as a reference to design ZBLAN PCF with different functions. Furthermore, we have optimized a circular lattice ZBLAN PCFs with 10 air hole rings were proposed to achieve low loss zero dispersion wavelength at 1.55 m, which was not achievable with 10 air hole rings uniform air hole ZBLAN CL-PCF.

We have shown the effect of the hole size closed to the core layer capable to control and shift the zero dispersion wavelength, dispersion value and slope polarity of ZBLAN PCF. In addition, we showed a ZBLAN PCF with near-zero flattened chromatic dispersion from 1.2–1.8μm wavelengths where the absolute dispersion variation is as small as 0.040 ps/nm/km from 1.2–1.8μm wavelength region.

Finally, supercontinuum generation (SC) around 1.55 μm is investigated with our proposed ZBLANCL-PCF. The simulations have been performed by solving the generalized nonlinear Schrödinger equation (NLSE) with a FWHM of 100 fs and peak power of 3.2 kW is employed. Results show that flat SC with a FWHM of 650 nm is successfully obtained for 20 cm of the CL PCF length.

References

[1] D. C. Tee , N. Tamchek and C. H. Raymond Ooi ,'' Numerical Modeling of the Fundamental Characteristics of ZBLAN Photonic CrystalFiber for Communication in 2–3μ m MidinfraredRegion'',IEEE photonics journal , Volume 8, Number 2, April 2016.

[2] Xin Jiang, Nicolas Y. Joly, Martin A. Finger, FehimBabic, Gordon K. L. Wong, John C. Travers1 and Philip St. J. Russell, *''Deep-ultraviolet to mid-infrared Supercontinuum generated in solid-core ZBLAN photonic crystal fiber''*, nature photonics , *19 January 2015* .

[3] W. Liu, S.A. Hosseini, Q. Luo, B. Ferland, S.L. Chin, O.G. Kosareva, N.A. Panov, and V.P. Kandidov, "*Experimental observation and simulations of the self-action of white light laser pulsepropagating in air*", New J. Phys. 6, (2004).

[4] N. Akozbek, A. Becker, M. Scalora, S.L. Chin, and C.M. Bowden, "*Continuum generation of thethird-harmonic pulse generated by an intense femtosecond IR laser pulse in air*", Appl. Phys, (2003).

[5] A.B. Fedotov, A.M. Zheltikov, A.A. Ivanov, M.V. Alfimov, D. Chorvat, V.I. Beloglazov, L.A. Melnikov, N.B. Skibina, A.P. Tarasevitch and D. von der Linde, "*Supercontinuum-generating holeyfibers as new broadband sources for spectroscopic applications*", Laser Phys, (2000).

[6] Y.E. Lozovik, A.L. Dobryakov, S.A. Kovalenko, S.P. Merkulova, S.Y. Volkov, and M. Willander, "*Study of localization of carriers in disordered semiconductors by femtosecondspectroscop*y", Laser Phys. (2002).

[7] MajidEbnali-Heidari,HamedSaghaei, FarshidKoohi-Kamali, Mohammad NaserMoghadasi,and Mohammad KazemMoravvej-Farshi,*" Proposal for Supercontinuum Generation byOptofluidic Infiltrated Photonic Crystal Fibers",*IEEE JOURNAL, SEPTEMBER/OCTOBER 2014.

[8] J.M. Dudley and J. R. Taylor, "*Supercontinuum generation in optical fibers*", Cambridge University Press, (2010)

[9] John M. Dudley, Laurent Provino, Nicolas Grossard, HervèMaillotte, Robert S. Windeler Benjamin J. Eggleton and StèphaneCoen, "*Supercontinuum generation in air–silica microstructuredfibers with nanosecond and femtosecond pulse pumping*", Journal of Optical Society of America, (2002).

[10] J. K. Ranka, R. S. Windeler and A. J. Stentz, "*Optical properties of high-delta air–silica microstructure optical fibers*", Optics Letters, (2000).

[11] J.M. Dudley and G. Genty, S. Coen, "*Supercontinuum generation in photonic crystal fiber*", Rev. Mod. Phys,(2006).

[12] Robert. R. Alfano, "*The Supercontinuum Laser Source: the ultimate white light*", Third edition,Springer, (2016).

[13] Benjamin Wetzel, "*Etudes expérimentales et numériques des instabilités non linéaires et desvagues scélérates optiques*", Thèse de doctorat, Franche-Comté University, (2012).

General Conclusion

The study reported in this thesis aims to analyze and optimize the propagation properties in the next generation of optical fibers commonly referred to as " Photonic Crystal Fibers (PCF), in our studies we used a photonic crystal fiber with a circular lattice based on ZBLAN instead of silica due to their transparent from 0.2 to 7.8 μm, in order to obtain a fiber with nearly zero ultra-flattened chromatic dispersion, for the use in supercontinuum generation.

The numerical simulation proves the impact of adjusting the opto-geometrical parameters of the fiber on the optical proprieties of the ZBLAN CL-PCF. The analysis of the individual results showed the possibility of determining values of the radius of the air holes of the microstructure to obtain the desired propagation characteristics. Using FDFD method, knowing that the large effective area fibers are generally multimodal, we demonstrated that only the fundamental mode can propagate in the heart with very low losses $2.3647.10^{-18}$ dB/km for λ=1.55 μm.

We found that the circular lattice ZBLAN PCF has a large effective area 11.176 μm^2, for the wavelength of 1.55 μm, with low losses of $2.3647.10^{-18}$ dB/km with nearly zero chromatic dispersion 0.040 ps.nm/km. in the end we completed our study with an analysis of the generation supercontinuum in PCF.

Finally, the numerical study, we have achieved during this thesis, we have improved understanding the guidance properties in the PCF and the impact of these different opto-geometrical parameters. In addition, the different results presented in this manuscript have shown the importance of numerical modeling in the study.